Effect of correlated decay on fault-tolerant quantum computation

B. Lemberger and D. D. Yavuz
Department of Physics, 1150 University Avenue, University of Wisconsin at Madison, Madison, Wisconsin 53706, USA
(Received 23 June 2017; published 29 December 2017)

We analyze noise in the circuit model of quantum computers when the qubits are coupled to a common bosonic bath and discuss the possible failure of scalability of quantum computation. Specifically, we investigate correlated (super-radiant) decay between the qubit energy levels from a two- or three-dimensional array of qubits without imposing any restrictions on the size of the sample. We first show that regardless of how the spacing between the qubits compares with the emission wavelength, correlated decay produces errors outside the applicability of the threshold theorem. This is because the sum of the norms of the two-body interaction Hamiltonians (which can be viewed as the upper bound on the single-qubit error) that decoheres each qubit scales with the total number of qubits and is unbounded. We then discuss two related results: (1) We show that the actual error (instead of the upper bound) on each qubit scales with the number of qubits. As a result, in the limit of large number of qubits in the computer, $N \to \infty$, correlated decay causes each qubit in the computer to decohere in ever shorter time scales. (2) We find the complete eigenvalue spectrum of the exchange Hamiltonian that causes correlated decay in the same limit. We show that the spread of the eigenvalue distribution grows faster with N compared to the spectrum of the unperturbed system Hamiltonian. As a result, as $N \to \infty$, quantum evolution becomes completely dominated by the noise due to correlated decay. These results argue that scalable quantum computing may not be possible in the circuit model in a two- or three- dimensional geometry when the qubits are coupled to a common bosonic bath.

DOI: 10.1103/PhysRevA.96.062337

I. INTRODUCTION

Over the past two decades, quantum computing and quantum information processing have emerged as exciting fields of science because of the possibility of solving certain problems much more quickly than any foreseeable classical computer [1–4]. It has been predicted that, in addition to factoring [5,6], quantum algorithms can be used for solving a variety of problems including efficient data search and finding the eigenvalues and eigenvectors of large matrices [7,8]. The most widely utilized model for quantum computing, which is often referred to as the circuit model, utilizes quantum bits (qubits) which are quantum systems that can be in two different states. Quantum computing relies on operations performed on qubits, analogous to gates on classical bits, but qubit operations can exploit the extraordinary behavior of nature at the quantum scale. The principles of quantum computing have now been demonstrated using a variety of physical qubits including trapped ions [9–11], neutral atoms [12–14], semiconductor quantum dots [15,16], superconductor Josephson junctions [17,18], and single photons [19,20]. Quantum mechanics tells us that the size of the Hilbert space of N identical two-level systems is 2^N, i.e., exponentially large in the number of qubits. Quantum computers are predicted to be so powerful in part because they utilize this exponentially large dimension of the Hilbert space and perform many computations simultaneously in parallel (often referred to as quantum parallelism). In this paper, we discuss a ubiquitous source of noise on quantum computers and argue the failure of scalability of quantum computation. This noise source is correlated (super-radiant) decay, which inevitably happens when the qubits are coupled to a common bosonic bath.

It is now well understood that the ideas of error correction and fault tolerance are central to any computer architecture, and quantum computers are no exception. Similar to our current silicon-based solid-state classical computers, future quantum computers will almost certainly employ codes to detect and correct errors at various stages of the computation. It is not *a priori* obvious that traditional error correction ideas would extend to quantum computers. Over the past two decades, a growing body of literature has shown that error correction and fault-tolerant operation is indeed possible for quantum computers [21–23]. One of the most important achievements in the field has been the discovery of the threshold theorem [24–28]. This theorem argues that if the quantum gates are constructed with a fidelity better than a certain threshold, then arbitrarily long quantum operations are, in principle, possible. The error threshold is typically established to be $\eta \sim 10^{-4}$, but can be as high as $\eta \sim 10^{-2}$ for surface codes [29]. The threshold theorem has been a main driving force in the field. Many experimental implementations of quantum computing have been aiming to demonstrate gate fidelities better than the mentioned threshold, in order to demonstrate the feasibility of their approach [9–20].

Although the threshold theorem is a remarkable achievement, it has a number of weaknesses. The theorem works under certain assumptions regarding the properties of the noise that affects the quantum computer. One of the key requirements is that the sum of the norms of the Hamiltonians that decoheres each qubit must be bounded. It is now well understood that this assumption is not valid for certain models of environment-qubit coupling, especially when the bath is bosonic in nature. In such cases, it has been discussed that the threshold theorem becomes extremely sensitive to the high-frequency spectrum of the bath operators [27]. A number of authors have also criticized the threshold theorem using more general arguments [30–33]. Despite these weaknesses, the threshold theorem has generally been regarded to cover most reasonable models of noise sources. Quantum computers are now widely believed to be scalable at least in principle, and the difficulties associated with constructing an actual quantum computer are considered technical in nature.

In this paper, we focus on the circuit model of quantum computation and analyze noise on quantum computers due to correlated decay between the qubit levels which inevitably happens when the qubits are coupled to a common bosonic bath [34]. We consider a two-dimensional (2D) or three-dimensional (3D) array of qubits and do not impose any restrictions on the size of the sample; i.e., the spacing between the qubits can be comparable to or larger than the emission wavelength. When the qubits are coupled to a common bosonic bath, the physical mechanism that causes correlated decay is the exchange interaction between the qubits. We first show that exchange interaction produces errors on each of the qubits that are outside the applicability of the threshold theorem. This is mainly because the strength of the exchange interaction between the qubits decays slowly as a function of their separation, and as a result, the introduced errors cannot be assumed local; each qubit in the computer is affected by the presence of any other qubit with a strength that violates the conditions of the threshold theorem. In more technical terms, the sum of the norms of the Hamiltonians that decoheres each qubit scales with the total number of qubits in the computer. This scaling is $N^{1/2}$ in a 2D and $N^{2/3}$ in a 3D geometry and the sum of the norms is not bounded in the $N \to \infty$ limit. Because the sum of the norms is unbounded, the introduced error on each qubit cannot be assumed lower than a certain threshold; this is precisely how the assumptions of the threshold theorem are violated.

The violation of the threshold theorem does not necessarily imply uncorrectable error in a quantum computer. The norm of a noise Hamiltonian is its largest eigenvalue, which can be viewed as an *upper bound* (i.e., the worst case scenario) for the introduced error. The fact that the upper bound cannot be assumed lower than a threshold does not necessarily imply the *actual* error in most instances of algorithm to be unbounded. We will discuss two results that argue that correlated decay indeed produces errors that are uncorrectable in the $N \to \infty$ limit. (1) We study the error on each qubit that is caused by correlated decay for a general state of the computer in the Hilbert space. Using two different methods, we find that for the vast majority of the Hilbert space, the actual error (instead of the upper bound) on each qubit scales with the total number of qubits in the computer. In the first method, we find the complete eigenvalue spectrum of the noise Hamiltonian that decoheres each qubit. In the second method, we use an iterative algorithm to solve for the time evolution of the reduced density matrix of each qubit. Both methods give the same answer and show that the single-qubit error scales as $\sqrt{\ln N}$ ($N^{1/6}$) in a 2D (3D) geometry. As a result, as $N \to \infty$, correlated decay causes each qubit in the computer to decohere in arbitrarily short time scales. (2) We find the complete eigenvalue spectrum of the total exchange Hamiltonian due to correlated decay. We show that in the $N \to \infty$ limit, the eigenvalues are distributed according to the Laplace distribution whose standard deviation (i.e., the spread) scales as $N^{1/2} \ln N$ ($N^{2/3}$) in a 2D (3D) geometry. As a result, the spread of the eigenvalues of the noise Hamiltonian scales faster with N compared to the unperturbed system Hamiltonian, which scales as $N^{1/2}$ in both geometries. This shows that in the $N \to \infty$ limit, the size of the noise Hamiltonian becomes much larger compared to the size of the unperturbed system Hamiltonian for the quantum system. As a result, the dynamics of the quantum evolution become completely dominated by the noise due to correlated decay.

As mentioned above, throughout this paper, we will focus on the limit of a large number of qubits in the computer, i.e., the limit $N \to \infty$. From a practical viewpoint, this limit may look purely academic without much real-world implication. However, many of the main ideas in modern computational complexity theory argue that this is not the case; the scaling in the $N \to \infty$ limit dictates in a very real and practical sense the efficiency of an algorithm [35]. It is now well understood that when the number of operations required to solve a certain problem scales polynomially with the problem size, then the problem is viewed as efficiently solvable. Such computational problems belong to the complexity class P and they are usually denoted by $P = T(\mathcal{N}^k)$ [here, $\mathcal{N}$ is some measure that is related to the size of the problem (for example, number of digits in factoring), and is usually polynomially related to the number of bits used]. When a polynomial algorithm cannot be found, then the problem is viewed as "hard" without an efficient algorithm to solve. The idea of polynomial scaling of the required number of operations (which can also be viewed as the run time of the algorithm) is central to the computational complexity theory. The question then is, from a practical viewpoint, why does polynomial scaling provide a crucial distinction? Suppose that we have two algorithms which scale as $\mathcal{N}^{1000}$ and $2^{0.001\mathcal{N}}$, respectively. From a purely practical viewpoint, for most reasonable instances of the problem, the second algorithm would require fewer steps to obtain the solution. Why would we then favor the first algorithm from a computational complexity standpoint? Although the answer to this question is not known for certain, more than 60 years of literature on the subject suggests that such pathological cases never happen [35]. The constants are irrelevant (i.e., $\mathcal{N}^k$ versus $2^{c\mathcal{N}}$ for arbitrary k and c), and the behavior as $\mathcal{N} \to \infty$ dictates the efficient solvability of a problem in practical instances. This is the key reason why it is important to understand the scalability and fault tolerance of quantum computers in the large number of qubits limit. This is also precisely the reason why it would be a mistake to ignore noise sources such as correlated decay by arguing that using proper choice of qubit levels (for example, clock states in neutral atoms) the decay time scales between the qubit levels can be quite long. Within this context, we would like to point out the pioneering work of Mucciolo and colleagues [36–39]. They analyzed fault-tolerant operation of quantum computers in detail when the qubits are coupled to a bosonic bath in the $N \to \infty$ limit (which they term as the thermodynamic limit). They have shown how time evolution of the system can be mapped onto a statistical spin model, and they have identified the existence of an error threshold with a thermodynamic-like phase transition. They have also clearly discussed the violation of the threshold theorem if the interactions are sufficiently long range. Our results are also related to the recent paper by Hutter and Loss, who have discussed the breakdown of error correction in surface codes during the presence of correlated noise [40]. Differing from what we will discuss below, they consider the propagation of errors at a certain point in the computer and discuss the scaling of the errors as a function of the depth of the computation (i.e., the number of quantum operations).

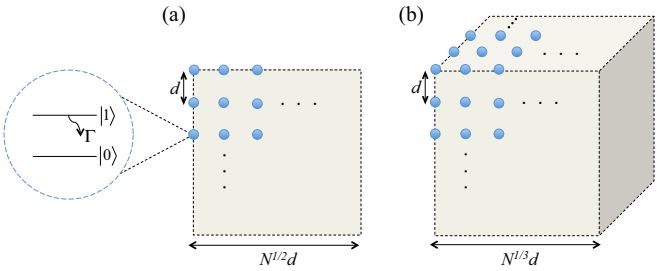

FIG. 1. We analyze an N-qubit quantum computer in (a) two- and (b) three-dimensional geometry with the qubits coupled to a common bosonic bath. For a single qubit present, the interaction with the bath causes an independent decay rate of Γ between the qubit levels. When the whole ensemble of qubits is present, correlated decay causes correlated errors to build up across the whole computer. Since we are primarily interested in the $N \to \infty$ limit, we do not impose restrictions on the size of the sample; i.e, the spacing between the qubits may be much larger than the radiation wavelength, $d \gg \lambda_a$. For concreteness, we focus on a square and a cube arrangement of atoms with regularly spaced qubits, but the results are not sensitive to the precise shape and arrangement structure of the array.

Throughout this paper, we will focus on the circuit model of quantum computation and will not consider other architectures such as adiabatic quantum computing [41]. Our results also do not apply to systems where the bath is fermionic in nature or where the interaction between the qubits and the bath is substantially different from the Hamiltonian of below Eq. (1), for example, to structures that are topologicaly protected [42]. Although our results argue that scalable quantum computing in the circuit model may not be possible in a 2D or 3D geometry when the qubits are coupled to a bosonic bath, we certainly have not proven that this is the case. It may perhaps be possible to overcome the noise that is described here by using clever encoding techniques (similar to decoherence-free subspaces [43–46]) or by designing the hardware appropriately (such as sufficiently isolating certain subsections of the computer so that the amount of correlations are reduced). We will discuss our preliminary assessment of a number of these strategies in the conclusions section.

II. FORMALISM AND THE EXCHANGE INTERACTION

Since the seminal paper by Dicke [47,48], the superradiance problem has been analyzed by a large number of authors and this problem continues to be relevant for a wide range of physical systems [49–58]. As shown in Fig. 1, we consider N two-level atoms, each with levels $|0\rangle$ and $|1\rangle$, in a two- or three-dimensional geometry. Throughout this paper, we will take all the qubits in the computer to be in the "causality cone," that is, sufficient time evolution is allowed so that each qubit in the computer can be causally influenced by every other qubit. In Fig. 1, for concreteness we have focused on square and cube geometries with a regular spacing of d between adjacent qubits. However, the results are insensitive to the precise shape of the geometry and also to the regular nature of the array (i.e., the qubits can be taken as randomly distributed within the considered region). We denote each individual qubit with the index j and consider a continuum of bosonic modes with annihilation and creation operators $\hat{a}_{\kappa\epsilon}$ and $\hat{a}^\dagger_{\kappa\epsilon}$ respectively. These operators act on the mode of the field with wave vector κ and polarization ϵ. The total Hamiltonian for the system when only the energy-conserving terms are retained (under the rotating-wave approximation) is

$$\begin{aligned}\hat{H}_{\text{total}} = &\sum_j \frac{1}{2}\hbar\omega_a \hat{\sigma}_z^j + \sum_{\kappa\epsilon}\hbar v_{\kappa\epsilon}\left(\hat{a}^\dagger_{\kappa\epsilon}\hat{a}_{\kappa\epsilon} + \frac{1}{2}\right)\\ &- \sum_j\sum_{\kappa\epsilon}\hbar g_{\kappa\epsilon}[\hat{a}_{k\epsilon}\exp(i\vec{\kappa}\cdot\vec{r}_j)\hat{\sigma}_+^j\\ &+ \hat{a}^\dagger_{\kappa\epsilon}\exp(-i\vec{\kappa}\cdot\vec{r}_j)\hat{\sigma}_-^j], \end{aligned} \tag{1}$$

where

$$\begin{aligned}\hat{\sigma}_z^j &= |1\rangle^j{}^j\langle 1| - |0\rangle^j{}^j\langle 0|,\\ \hat{\sigma}_+^j &= |1\rangle^j{}^j\langle 0|,\\ \hat{\sigma}_-^j &= |0\rangle^j{}^j\langle 1|. \end{aligned} \tag{2}$$

In Eq. (1), the first two terms describe the qubit array and the bosonic modes in the absence of any interaction whereas the third term describes the coupling between the two systems. $\vec{r}_j$ is the position of the jth atom and the energies of the qubit states $|0\rangle$ and $|1\rangle$ are taken to be $-\frac{1}{2}\hbar\omega_a$ and $\frac{1}{2}\hbar\omega_a$, respectively. The Dicke limit of the above equations is obtained when the total size of the sample is assumed to be small compared to the κ vector of the relevant modes, i.e., $\vec{\kappa}\cdot\vec{r}_j \to 0$. It is now well understood that the key physical effect that describes many different aspects of correlated decay and super-radiance is the exchange interaction. Starting with the Hamiltonian of Eq. (1), this interaction has been derived using a variety of approaches by a number of authors [59–62]. One such derivation of the exchange interaction Hamiltonian is shown in Appendix A. This derivation uses assumptions that are similar to the traditional Wigner-Weisskopf theory of spontaneous decay [63]. Briefly, we take the initial atomic system to be an arbitrary superposition (in general entangled state) and assume initially zero excitation in each bosonic mode $\kappa\epsilon$. We then study the problem in the interaction picture and integrate out the probability amplitudes of the continuum states using the usual Born-Markov approximation. Using this approach, the end result is the following effective interaction Hamiltonian:

$$\hat{H}_{\text{eff}} = \sum_j\sum_k \hat{H}^{jk}. \tag{3}$$

Here, the sum is over all pairs of qubits and operators $\hat{H}^{jk}$ act nontrivially only on the qubits with indices j and k

$$\hat{H}^{jk} = F_{jk}\hat{\sigma}_+^j\hat{\sigma}_-^k + F_{kj}\hat{\sigma}_-^j\hat{\sigma}_+^k, \tag{4}$$

which is essentially a "spin" exchange interaction (mediated by photon modes) with coupling constants of F_{jk}:

$$\begin{aligned}F_{jk} = F_{kj} = -\left(i\frac{\Gamma}{2} + \delta\omega\right)\left(\frac{3}{8\pi}\right)\Bigg[&4\pi(1-\cos^2\theta_{jk})\frac{\sin\kappa_a r_{jk}}{\kappa_a r_{jk}}\\ &+ 4\pi(1-3\cos^2\theta_{jk})\left(\frac{\cos\kappa_a r_{jk}}{(\kappa_a r_{jk})^2} - \frac{\sin\kappa_a r_{jk}}{(\kappa_a r_{jk})^3}\right)\Bigg]. \end{aligned} \tag{5}$$

Here, Γ is the single-atom decay rate and $\delta\omega$ is the single-atom Lamb shift of the qubit transition. r_{jk} is the distance between the two atoms, and θ_{jk} is the angle between the atomic dipole moment vector and the separation vector $\vec{r}_{jk}$. The quantity κ_a is the wave vector for the bosonic modes energy resonant with the qubit transition: $\kappa_a = \omega_a/c$. For concreteness, we have focused on qubits in free space interacting with electromagnetic modes and have taken the nature of the qubit transition to be dipolar (electric or magnetic dipole). However, the scaling results that we discuss would apply to other types of radiation, such as quadrupole or higher order multipole, with only the angular factors in Eq. (5) being different. Similarly, the formalism would also apply to other types of bosonic baths, such as phonons in solid-state structures. Note that the coupling constants F_{jk} are complex with an imaginary part proportional to single-atom decay rate Γ. As a result, the effective Hamiltonian of Eq. (3) is not Hermitian since it models dissipative decay in addition to unitary dynamics. For the below discussion, the precise values of the constants F_{jk} are not important. Rather, two properties of these constants are critical: (i) they have random signs for large separation of the qubits, $\kappa_a r_{jk} \gg 1$, and (ii) to leading order, they scale as $F_{jk} \propto 1/\kappa_a r_{jk}$. All the scaling behavior with respect to the total number of qubits will result from these two properties. Similarly, the non-Hermiciticity of the effective Hamiltonian of Eq. (3) is also not of significance. Our scaling results would remain identical if we ignore the decay part of the problem and only focus on resonance shifts due to the exchange interaction (i.e., if we ignore the imaginary parts of the coupling constants of Eq. (5) and take them to be purely real).

Born-Markov approximation that results in the effective exchange Hamiltonian of Eq. (3) assumes the evolution time scales for the state coefficients to be slow compared to the correlation time scales of the bath. As we will discuss below, decoherence time scales will get shorter as $N \to \infty$, and for a sufficiently large N, the assumptions of the Born-Markov approximation will be violated. When Born-Markov approximation is not satisfied, the system can no longer be described by the static Hamiltonian of Eq. (3); instead the rate of change in each state coefficient is not only influenced by the values of the other coefficients at that particular time but depend on their evolution history. All the scaling results that we discuss in the paper result from N-dependent sums over coupling constants between the state coefficients, which have almost random phases (due to large spacings) and $1/r_{jk}$ scaling factors. As a result, the scaling results should not be altered when one considers not just the values of the coefficients at that particular time but also their evolution history, since neither phases nor the average strengths of the coupling constants are altered. We will discuss the extension of our formalism beyond the Born-Markov approximation also in Appendix A.

III. VIOLATION OF THE THRESHOLD THEOREM

We next discuss how the effective Hamiltonian of Eq. (3) violates the threshold theorem. We note that the exchange Hamiltonian involves two-qubit interactions only, and the applicability of the threshold theorem under these conditions is well understood. Following Ahoronov and colleagues [26–28], each qubit j decoheres with the Hamiltonian $\hat{H}^j \equiv \sum_k \hat{H}^{jk} = \sum_k F_{jk}\hat{\sigma}_+^j\hat{\sigma}_-^k + F_{kj}\hat{\sigma}_-^j\hat{\sigma}_+^k$ (which we will frequently refer to as the single-qubit error Hamiltonian). An upper bound on the magnitude of the error can be found using the inequality $\|\sum_k \hat{H}^{jk}\| < \sum_k \|\hat{H}^{jk}\|$ (the notation $\|\ldots\|$ denotes the L_2 operator norm). The applicability of the threshold theorem then requires

$$\sum_k \|\hat{H}^{jk}\| t_0 < \eta, \tag{6}$$

where t_0 is the time required for a quantum gate. Equation (6) requires the sum of operator norms to be bounded, $\sum_k \|\hat{H}^{jk}\| < \infty$. We note that for the exchange interaction the operator norm for each pair Hamiltonian is given by the absolute value of the coupling constants, $\|\hat{H}^{jk}\| = |F_{jk}|$. As a result, for the threshold theorem to be applicable, we would require $\sum_k |F_{jk}| < \infty$. However, in both 2D and 3D geometries this sum scales with the number of qubits and is unbounded. In a 3D geometry, the distance between the qubits scales as $r_{jk} \propto N^{1/3}d$. Since there are N terms in the sum of operator norms, we have, to leading order, $\sum_k |F_{jk}| \propto (\Gamma/\kappa_a d)N^{2/3}$. In a 2D geometry for the qubit array, the spacing between the qubits scales as $r_{jk} \sim N^{1/2}d$, and the corresponding scaling for the sum of the operator norms is $\sum_k |F_{jk}| \propto (\Gamma/\kappa_a d)N^{1/2}$. Physically, the key reason for the violation of the threshold theorem in both two and three dimensions is that the interaction strength between the qubits due to correlated-decay drops slowly as a function of distance, only as $\propto 1/r$.

We note that as the spacing between the qubits d is increased, the correlated error and the sum of the norms would drop as $\sum_k |F_{jk}| \propto 1/\kappa_a d$. This may initially suggest that the noise due to correlated decay can be reduced to arbitrarily low values by increasing the separation between the qubits. However, this argument is misleading since, as shown in Eq. (6), the important quantity is the amount of error during the time required for a quantum gate t_0. As the qubits become further apart, the two-qubit gate time will increase at least as $t_0 \propto d/c$ (due to fundamental causality constraint). As a result, the amount of error per gate time due to correlated decay is independent of the qubit separation d.

IV. SINGLE-QUBIT ERROR

The violation of the threshold theorem does not necessarily imply uncorrectable error. The reason is that the norm of an operator is its largest eigenvalue and the sum of the norms in Eq. (6) can be viewed as an upper bound, i.e., the worst-case scenario for the error. This worst-case scenario may occur only in a specific region of the Hilbert space with a dimension that does not grow exponentially with N. In this case, for most states of the quantum computer, the introduced errors will not scale with the number of qubits, allowing for error correction. Calculating the actual error on the qubits instead of just the upper bound is a much more difficult task since it requires finding the complete eigenvalue spectrum of the error Hamiltonian (instead of just the largest eigenvalue). In this section, we accomplish this goal by explicitly evaluating all the moments of the eigenvalue distribution in the $N \to \infty$ limit. With the moments of the distribution calculated, we find the complete eigenvalue spectrum of the single-qubit

error Hamiltonian and show that the width of the eigenvalue distribution scales with the number of qubits. This scaling is $\sqrt{\ln N}$ in a 2D geometry and $N^{1/6}$ in a 3D geometry, and as expected, it grows more slowly with the number of qubits compared to the scaling of the largest eigenvalue. Because of this scaling, in the $N \to \infty$ limit, the errors on each qubit would happen in arbitrarily short time scales, rendering error correction impossible. The very slow $\sqrt{\ln N}$ scaling in a 2D case suggests that this geometry may be on the threshold of scalability for noise due to correlated decay.

We have also been able to verify these results by calculating the dynamics of the reduced density matrix for a specific qubit. We find an analytical solution for the evolution of the reduced density matrix under the single-qubit error Hamiltonian which is valid in the $N \to \infty$ limit. Consistent with the eigenvalue spectrum discussed in the previous paragraph, this solution predicts decoherence of each qubit with a time scale that gets shorter with the mentioned scalings ($\sqrt{\ln N}$ in a 2D and $N^{1/6}$ in a 3D geometry). We have also found that this analytical solution predicts the dynamics reasonably well even for a computer with a relatively low number of qubits. As we discuss below, we perform exact numerical calculations for a 16-qubit quantum computer and show good agreement between analytical results and the numerical simulations.

A. Eigenvalue spectrum of the single-qubit error Hamiltonian

In this section, we discuss the complete eigenvalue spectrum of the single-qubit error Hamiltonian $\hat{H}^j = \sum_k \hat{H}^{jk} = \sum_k F_{jk}\hat{\sigma}_+^j\hat{\sigma}_-^k + F_{kj}\hat{\sigma}_-^j\hat{\sigma}_+^k$ in the $N \to \infty$ limit. In this limit, the eigenvalues λ of $\hat{H}^j$ can be viewed as having a continuous distribution with probability density function $f_\Lambda(\lambda) \equiv P\{\Lambda = \lambda\}$. This probability density function can be evaluated by explicitly calculating all the moments of the distribution $\sigma^{(m)} \equiv E[\Lambda^m] = \int f_\Lambda(\lambda)\lambda^m d\lambda$, where $E[\ldots]$ stands for the expected value. By definition, these moments are

$$\sigma^{(m)} = E[\Lambda^m] = 2^{-N}\mathrm{Tr}[(\hat{H}^j)^m]. \tag{7}$$

Remarkably, we were able to analytically calculate all the moments using Eq. (7) in the $N \to \infty$ limit and thereby explicitly evaluate $f_\Lambda(\lambda)$. This derivation is shown in detail in Appendix B. Here, we give a brief summary of the main ideas used in this derivation. For all integers m, the trace can be explicitly evaluated using $\hat{H}^j = \sum_k \hat{H}^{jk}$:

$$\begin{aligned}\sigma^{(m)} &= 2^{-N}\mathrm{Tr}[(\hat{H}^j)^m] = 2^{-N}\sum_q \langle q|(\hat{H}^j)^m|q\rangle \\ &= 2^{-N}\sum_q\sum_{k_1}\cdots\sum_{k_m}\langle q|\hat{H}^{jk_1}\ldots\hat{H}^{jk_m}|q\rangle, \end{aligned}\tag{8}$$

where the state $|q\rangle$ runs through all 2^N possible combinations of the qubit basis states. Using Eq. (8), calculating the trace is reduced to summing over the matrix elements of the products of two-qubit exchange Hamiltonians $\hat{H}^{jk}$. We first observe that in order for $\langle q|\hat{H}^{jk_1}\ldots\hat{H}^{jk_m}|q\rangle \neq 0$, each $\hat{H}^{jk_i}$ must appear an even number of times; thus if m is odd, $\sigma^{(m)} = 0$. For m even, in the high-N limit the trace is dominated by the terms which correspond to sequences of Hamiltonians $\hat{H}^{jk_1}\ldots\hat{H}^{jk_m}$ (which we identify with the sequence of qubits $\{k_1\ldots k_m\}$) in which each qubit k_i appears exactly twice. This is discussed in detail in Appendix B. Because the status of qubit j alternates as the two-qubit Hamiltonians are applied to $|q\rangle$, if the first Hamiltonian $\hat{H}^{jk_i}$ at which a given qubit k_i appears is at an even (odd) location in the sequence, then the second time the same Hamiltonian $\hat{H}^{jk_i}$ appears must be at an odd (even) location. These sequences correspond to ways to pair the Hamiltonians at an even location in the sequence, of which there are $m/2$, with Hamiltonians at odd locations, of which there are also $m/2$. Thus there are $(m/2)!$ ways to pair them, and we call such a pairing s, so that the sum over all of these pairings is $\sum_s$ (note that here, differing from in Appendix B, in order to simplify the discussion we have chosen the patterns s to be not ordered).

For a given pairing s, a sequence can be reconstructed by choosing a set of qubits $\{k_1\ldots k_{m/2}\}$ and an order to assign them to the pairs. For concreteness, consider $m = 6$ and the specific sequence of Hamiltonians $\hat{H}^{j,5}\hat{H}^{j,31}\hat{H}^{j,31}\hat{H}^{j,5}\hat{H}^{j,2}\hat{H}^{j,2}$. This sequence can be broken down into the pattern {{1,4},{2,3},{5,6}} (labelling the leftmost Hamiltonian 1 and the rightmost as 6) and the qubit list {5,31,2}. All relevant sequences conform to exactly one pairing s, and all sequences which conform to a pairing are accounted for by summing over all ways to assign qubits to those pairings, i.e., $\sum_{\{k_1\ldots k_{m/2}\}}$.

For any sequence s, the number of q for which $\langle q|\hat{H}^{jk_1}\ldots\hat{H}^{jk_m}|q\rangle \neq 0$ is $2^{N-m/2}$, because the status of each of the qubits $\{k_1\ldots k_m\}$ is fixed relative to j, and modifying the status of any other qubit preserves $\langle q|\hat{H}^{jk_1}\ldots\hat{H}^{jk_m}|q\rangle$. Because each qubit appears twice in $\{k_1\ldots k_m\}$, there are only $m/2$ qubits in that list, leaving $N - m/2$ other qubits which each can be up or down. For example, consider the sequence and state $\langle q|\hat{H}^{j,5}\hat{H}^{j,31}\hat{H}^{j,31}\hat{H}^{j,5}\hat{H}^{j,2}\hat{H}^{j,2}|q\rangle \neq 0$ with $m = 6$; it must be that qubit 2 is opposite j in q (i.e., if j is raised in q then 2 is lowered, or vice versa), qubit 5 must also be opposite j, and qubit 31 must match j. Thus once j is fixed, the three (or more generally $m/2$) qubits involved in the sequence are fixed, while the other $N - 1 - 3 = N - 1 - m/2$ are arbitrary. There are two choices for j, as well as for the other $N - 1 - 3 = N - 1 - m/2$ qubits, leading to $2 \times 2^{N-1-3} = 2^{N-3} = 2^{N-m/2}$ states.

For each of the q for which $\langle q|\hat{H}^{jk_1}\ldots\hat{H}^{jk_m}|q\rangle \neq 0$, this matrix element is simply the product of exchange coupling constants $\langle q|\hat{H}^{jk_1}\ldots\hat{H}^{jk_m}|q\rangle = F_{jk_1}^2\ldots F_{jk_{m/2}}^2$. Therefore, if we break up the sum over sequences which conform to the condition that each qubit appears exactly twice into a sum over pairings s and qubit assignments $\{k_1\ldots k_{m/2}\}$, we obtain

$$\sigma^{(m)} = 2^{-N}2^{N-m/2}\sum_s\sum_{\{k_1\ldots k_{m/2}\}} F_{jk_1}^2\ldots F_{jk_{m/2}}^2. \tag{9}$$

There is no s dependence to the right of its sum, so it simply contributes a multiplication by the number of pairings s, which is $(m/2)!$ as previously discussed. As discussed in detail in Appendix B, in the high-N limit the second sum can be replaced by the expected value of the exchange coupling constants and a combinatorial factor $\sum_{\{k_1\ldots k_{m/2}\}} F_{jk_1}^2\ldots F_{jk_{m/2}}^2 \to \binom{N-1}{m/2}(m/2)!E'[F^2]$ (here, $E'[..]$ denotes the expected value of the quantity in brackets over all pairings jk with j fixed). Using the high-N limit of the combinatorial prefactor $[\binom{N-1}{m/2}(m/2)! \to N^{m/2}]$, we finally

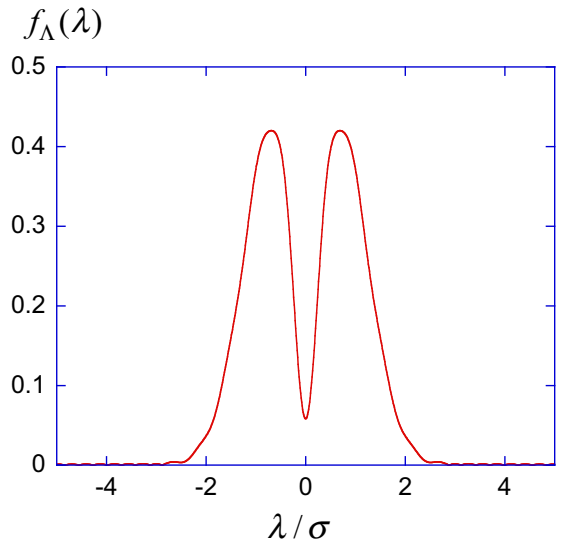

FIG. 2. The distribution of the eigenvalues of the single-qubit error Hamiltonian $\hat{H}^j = \sum_k \hat{H}^{jk} = \sum_k F_{jk}\hat{\sigma}_+^j\hat{\sigma}_-^k + F_{kj}\hat{\sigma}_-^j\hat{\sigma}_+^k$ in the $N \to \infty$ limit. The distribution has a width $\sigma = (NE'[F^2]/2)^{1/2}$ (the quantity $E'[F^2]$ denotes the expected value of the square of the coupling constants for all pairings jk with j fixed), which scales as $\sigma \sim \sqrt{\ln N}$ in a 2D and $\sigma \sim N^{1/6}$ in a 3D geometry, respectively.

obtain

$$\begin{aligned} \sigma^{(m)} &\to (m/2)!(NE'[F^2]/2)^{m/2} && m \text{ even}, \\ \sigma^{(m)} &= 0 && m \text{ odd}. \end{aligned} \tag{10}$$

Equation (10) shows that the probability density function has a standard deviation $\sigma = (NE'[F^2]/2)^{1/2}$. Using the expected values of the coupling constants as discussed in Appendix E, the width of the distributions would scale as $\sigma \sim \sqrt{\ln N}$ in 2D and $\sigma \sim N^{1/6}$ in 3D, respectively. The moments shown in Eq. (10) do not correspond to any known distribution. However, using these moments, we can find the probability density function $f_\Lambda(\lambda)$ by first calculating the moment generating function:

$$\begin{aligned} F_{\text{moment}}(\zeta) &\equiv E[\exp(i\zeta\Lambda)] \\ &= \int \exp(i\zeta\lambda) f_\Lambda(\lambda) d\lambda \\ &= E\left[1 + i\zeta\Lambda + \frac{(i\zeta)^2}{2!}\Lambda^2 + \cdots\right] \\ &= 1 + \sum_{m \text{ even}} (-1)^{m/2}(m/2)!\frac{(\sigma\zeta)^m}{m!}. \end{aligned} \tag{11}$$

With the moment generating function calculated using Eq. (11), the probability density function can then be estimated by taking the inverse Fourier transform $f_\Lambda(\lambda) = \int F_{\text{moment}}(\zeta)\exp(-i\zeta\lambda)d\zeta$. We perform this calculation numerically by using all the even moments m ranging from 2 to 200 in Eq. (11). The calculated probability density function $f_\Lambda(\lambda)$ with the horizontal axis scaled by the standard deviation of the distribution is shown in Fig. 2.

We next discuss how the eigenvalue distribution of the single-qubit error Hamiltonian relates to the single-qubit error. The state of the computer can be written as a superposition of the eigenstates of the single-qubit error Hamiltonian, $|\psi\rangle = \sum_n c_n|v_n\rangle$. The error on the state vector over a gate time t_0 will then be $\epsilon \sim \sqrt{\sum_n |c_n|^2\lambda_n^2}t_0 \sim \sigma t_0$. Since the width of the distribution of the eigenvalues, σ, scales with the number of qubits, the actual error also scales with the number of qubits for the vast majority of the states of the quantum computer in the Hilbert space. More formally, if we bound the amount of single-qubit error by a threshold, $\epsilon < \eta$, the fraction of the Hilbert space producing errors below this bound vanishes as $N \to \infty$.

B. Time evolution of the reduced density matrix

In this section, we discuss the time dynamics of the reduced density matrix for a specific qubit in the ensemble, qubit j. In this section only, we take the exchange coupling constants F_{jk} to be purely real and consider Hermitian dynamics (i.e., we focus on the Lamb shift part of the coupling constants instead of the decay). One motivation for this simplification is to emphasize that all the scaling results that we discuss do not rely on the non-Hermiciticity of the exchange Hamiltonian. Also, non-Hermitian dynamics cause the probability amplitudes to be not conserved, which complicates interpretation of the dynamics. Without loss of generality, we can write the initial state of the computer in the following form:

$$|\psi(t=0)\rangle = |0\rangle^j \otimes \sum_q \alpha_q|q\rangle + |1\rangle^j \otimes \sum_q \beta_q|q\rangle. \tag{12}$$

Here, differing from the rest of the paper, $|q\rangle$ denotes the states of the remaining $N-1$ qubits other than that specific qubit j (instead of the state of the full computer), and the quantities α_q and β_q are the complex expansion coefficients. Using the single-qubit error Hamiltonian $\hat{H}^j = \sum_k \hat{H}^{jk}$ and the expansion of Eq. (12), Schrodinger's equation can be reduced to a set of coupled differential equations for the coefficients:

$$i\frac{d\alpha_q}{dt} = \sum_k F_{jk}^*\beta_{q\ominus k}, \quad i\frac{d\beta_q}{dt} = \sum_k F_{jk}\alpha_{q\oplus k}. \tag{13}$$

Here, we use the notation $|q \ominus k\rangle$ to mean the configuration that equals $|q\rangle$ at all qubits except qubit $k \neq j$ which has undergone $|1\rangle^k \to |0\rangle^k$ transition (the summation is over configurations $|q \ominus k\rangle$ where $|q\rangle$ has qubit k raised). Similarly, $|q \oplus k\rangle$ is the configuration that equals $|q\rangle$ at all qubits except qubit $k \neq j$ which has undergone $|0\rangle^k \to |1\rangle^k$ transition. With the time evolution for the coefficients calculated through Eq. (13), the reduced density matrix elements for the qubit j can be calculated by writing out the full density matrix and tracing out the coordinates of the remaining $N-1$ qubits, which results in $\rho_{00}^j(t) = \sum_q |\alpha_q(t)|^2$, $\rho_{11}^j(t) = \sum_q |\beta_q(t)|^2$ (the diagonal density matrix elements), and $\rho_{01}^j(t) = \sum_q \alpha_q(t)\beta_q^*(t)$ (the off-diagonal density matrix element).

We first discuss the solution of Eqs. (13) when the initial condition is such that only one of the α_Q coefficients for a specific configuration Q is nonzero [i.e., $\alpha_Q(t=0) = 1$; $\alpha_q(t=0) = 0$ for $q \neq Q$; $\beta_q(t=0) = 0$]. The key difficulty in finding the solution is that due to the structure of the coupled equations (Fig. 3), the number of coefficients that α_Q couples to grows exponentially. For the vast majority of states Q in the Hilbert space, α_Q initially couples to ($\sim N/2$) $\beta_{Q\ominus k}$ coefficients, each of which couples to ($\sim N/2$) $\alpha_{Q\ominus k\oplus k'}$

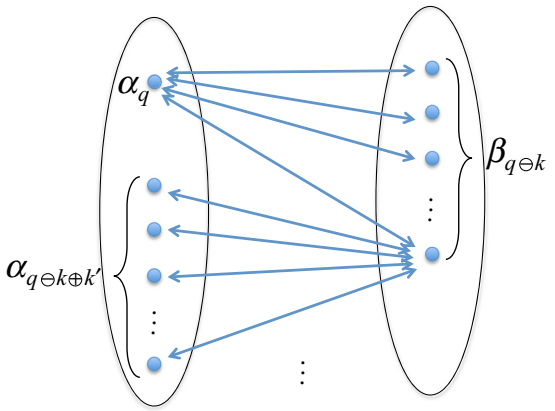

FIG. 3. The structure of the couplings in the coupled equations of Eqs. (13). Each α_q initially couples to $(\sim N/2)$ $\beta_{q\ominus k}$ coefficients, each of which couples to $(\sim N/2)$ $\alpha_{q\ominus k\oplus k'}$ coefficients, and this structure continues until α_q couples to all the coefficients in a specific subspace of the Hilbert space. Because of this nested structure, the number of coefficients that α_q couples to grows exponentially.

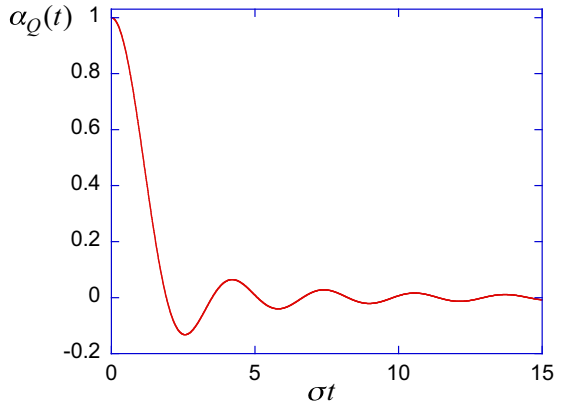

FIG. 4. The evolution of $\alpha_Q(t)$ as a function of time for the initial condition $\alpha_Q(t=0)=1$; $\alpha_q(t=0)=0$ for $q\neq Q$; $\beta_q(t=0)=0$. The initial probability amplitude decays in time scales given by $t\propto 1/\sigma$, where $\sigma=(NE'[F^2]/2)^{1/2}$. As a result, the decay time scale gets ever shorter as the total number of qubits in the computer is increased: $t\sim 1/\sqrt{\ln N}$ in 2D, $t\sim 1/N^{1/6}$ in 3D, respectively.

coefficients, each of which couples to $(\sim N/2)$ $\beta_{Q\ominus k\oplus k'\ominus k''}$ coefficients, and this nested structure continues. This structure suggests that an iterative solution based on Taylor series expansion can be found. The details of this solution are discussed in Appendix C. Briefly, we start with the zeroth-order solution, which is essentially the initial condition (at $t=0$) for the coefficients: $\alpha_Q^{(0)}=1$; $\alpha_q^{(0)}=0$ for $q\neq Q$; $\beta_q^{(0)}=0$. We then solve Eqs. (13), using the zeroth-order solutions on the right-hand side of the equations. The result gives us the first-order solutions which we denote as $\alpha_Q^{(1)}$, $\alpha_q^{(1)}$, and $\beta_q^{(1)}$. These first-order solutions are then used to resolve the coupled differential equations to give second-order solutions, and this iterative procedure is repeated until all orders of the Taylor series expansion are found. The end result is a Taylor series solution of the form

$$\alpha_Q(t)=\sum_n(-1)^n\frac{l(n)}{(2n)!}(\sigma t)^{2n}, \tag{14}$$

where σ is the standard deviation of the eigenvalue distribution of the single-qubit error Hamiltonian as discussed above $\sigma=(NE'[F^2]/2)^{1/2}$. The quantities $l(k)$ are combinatorial factors whose values are calculated algebraically using an iterative algorithm which gives $l(1)=1, l(2)=2, l(3)=5, l(4)=14$, $l(5)=42$, $l(6)=132$, and so on. The details of this iterative algorithm can also be found in Appendix C. We numerically find that the Taylor series converges when more than about 30 terms are kept in the expansion (i.e., terms that go until t^{60}). Using this approach, we numerically evaluate $\alpha_Q(t)$ and the result is shown in Fig. 4. $\alpha_Q(t)$ decays as the amplitude leaks out to the other states in the Hilbert space in time scales $t\propto 1/\sigma$. As discussed above, the standard deviation of the eigenvalue distribution scales as $\sigma\sim\sqrt{\ln N}$ in a 2D geometry and $\sigma\sim N^{1/6}$ in a 3D geometry, respectively. As a result, the decay time scale gets ever shorter as the total number of qubits in the computer is increased: $t\sim 1/\sqrt{\ln N}$ in 2D, $t\sim 1/N^{1/6}$ in 3D, respectively.

To extend the analysis to an arbitrary initial state, we utilize the linearity of the problem. We denote the specific time function that starts at a value of 1 and decays to 0 as plotted in Fig. 4 with $\xi(t)$. In the previous paragraphs, we have shown that with $\alpha_Q(t=0)=1$ initial condition, the solution is of the form $\alpha_Q(t)=\alpha_Q(t=0)\xi(t)$. Using the general form of the solution of the Schrodinger's equation, $|\psi(t)\rangle=\exp(-i\hat{H}^j t)|\psi(t=0)\rangle$, for an arbitrary initial state written in the form of Eq. (12), the solutions for the expansion coefficients will be of the form

$$\begin{aligned}\alpha_q(t)&=\alpha_q(t=0)\xi(t)+\delta\alpha_q(t),\\ \beta_q(t)&=\beta_q(t=0)\xi(t)+\delta\beta_q(t).\end{aligned} \tag{15}$$

Here, $\delta\alpha_q(t)$ and $\delta\beta_q(t)$ include the "flow" of the probability amplitude to that specific α_q or β_q due to the decay of all the other coefficients. The key insight that Eq. (15) gives is that each coefficient in the initial condition decays with the time function $\xi(t)$ and gets gradually replaced by a "random-looking" contribution that depends in a complex manner on all the other coefficients. This shows that the function $\xi(t)$ as plotted in Fig. 4 captures the "single-qubit error." For example, the evolution of one of the off-diagonal density matrix element (coherence) for this specific qubit j is given by

$$\begin{aligned}\rho_{01}^j(t)&=\sum_q\alpha_q(t)\beta_q^*(t)\\ &=\sum_q\alpha_q(0)\beta_q^*(0)\xi(t)^2+\sum_q\alpha_q(0)\delta\beta_q^*(t)\xi(t)\\ &\quad+\sum_q\delta\alpha_q(t)\beta_q^*(0)\xi(t)+\sum_q\delta\alpha_q(t)\delta\beta_q^*(t)\\ &=\rho_{01}^j(0)\xi(t)^2+\sum_q\alpha_q(0)\delta\beta_q^*(t)\xi(t)\\ &\quad+\sum_q\delta\alpha_q(t)\beta_q^*(0)\xi(t)+\sum_q\delta\alpha_q(t)\delta\beta_q^*(t).\end{aligned} \tag{16}$$

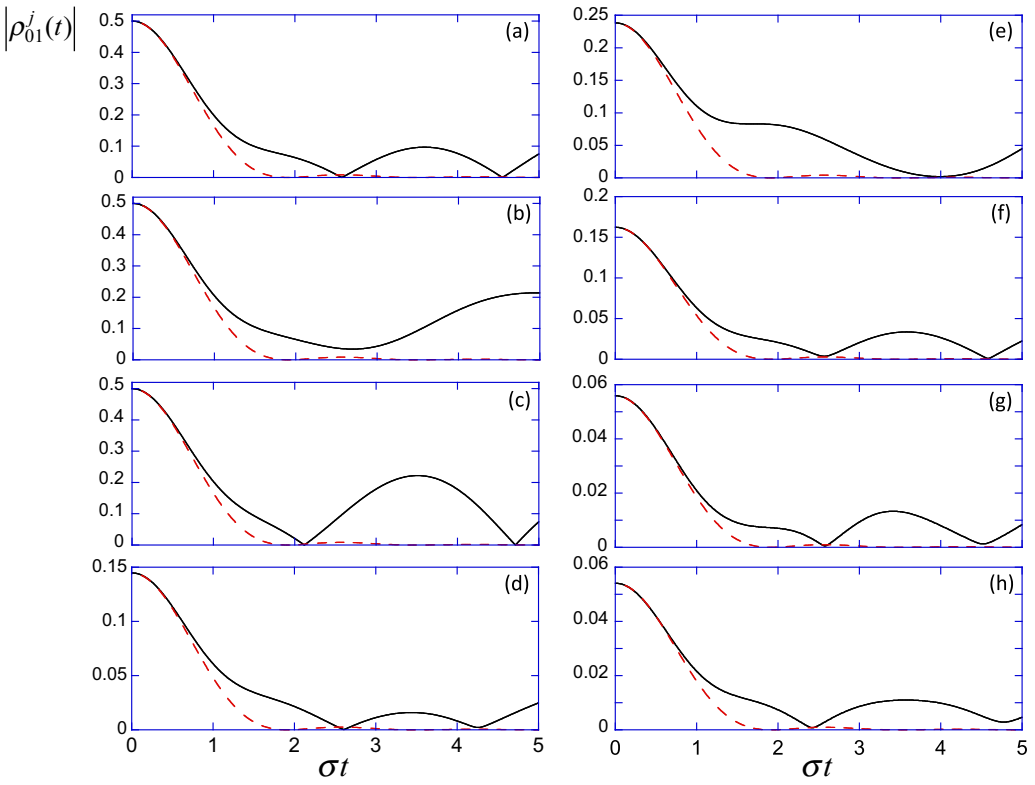

FIG. 5. The time evolution of the coherence (off-diagonal density matrix element) for qubit j, $\rho_{01}^{j}(t)$, for eight different initial conditions in a 16-qubit quantum computer. (a) Uniform initial condition $\alpha_q(t=0)=\beta_q(t=0)=1/\sqrt{2^N}$, (b) 8 nonzero amplitudes with equal amplitudes and phases, (c) only 2 nonzero amplitudes, (d) 200 nonzero amplitudes with 50 of them π out of phase with the rest, (e) 50 nonzero amplitudes with 8 of them π out of phase with the rest, and [(f)–(h)] all nonzero probability amplitudes with random amplitudes and phases (slight nonrandomness in the phases is introduced to produce a small initial value of the single-qubit coherence). For comparison, the square of the analytical solution of Fig. 4 is also plotted for each initial condition (red dashed line). The initial decay is well predicted by the analytical solution (which is valid in the $N\to\infty$ limit) even for this low number of qubits.

Equation (16) shows that the initial coherence for the qubit decays with the function $\xi(t)^2$ and gets replaced by sums over quantities that involve $\delta\alpha_q(t)$ and $\delta\beta_q(t)$. In the $N\to\infty$ limit, the coupling coefficients F_{jk} have practically random signs. As a result, the signs of $\delta\alpha_q(t)$ and $\delta\beta_q(t)$ are also random, and neither of the three sums in Eq. (16) produce substantial coherence. This shows that qubit j decoheres and essentially loses all the information regarding its initial coherence in time scales determined by $t\propto 1/\sigma$. The evolution of the diagonal density matrix elements, ρ_{00}^{j} and ρ_{11}^{j}, would show exactly the same behavior. The bit-flip errors would also happen in time scales determined by $t\propto 1/\sigma$.

We have also tested these ideas by performing numerical simulations over the full Hilbert space of the computer. In these simulations, starting with a specific initial state, we numerically solve coupled equations of Eqs. (13) using the finite difference method on a discrete time grid. Because of memory limitations, the largest number of atoms that we can simulate is limited to 16 with the Hilbert space dimension of $2^{16}=65536$. For concreteness, we consider a 2D 4×4 array of qubits and choose qubit j to be at the corner of the array. We take the emission wavelength to be $\lambda_a=9$ and choose $d=5$ in arbitrary units such that $\kappa_a d=10\pi/9$. Figure 5 shows the evolution of the coherence for the qubit j, ρ_{01}^{j}, for eight different initial conditions; the specifics of these initial conditions are outlined in the figure caption. For all eight of these initial conditions, the initial decay of the coherence is rather similar. Because of the low number of qubits considered, the values of the coupling constants F_{jk} do not span a very large range. As a result, there are partial revivals of the coherence at time points that depend on the specifics of the initial conditions. For comparison, the square of the analytical solution of Fig. 4, $\xi(t)^2$, is also plotted for each initial condition (red dashed line). The initial decay is well predicted by the analytical solution, which is strictly speaking valid in the $N\to\infty$ limit. Using similar numerical simulations with a variety of initial conditions, we have also looked at the evolution of the diagonal density matrix elements for qubit j, $\rho_{11}^{j}(t)$, and $\rho_{00}^{j}(t)$. We have found results to be similar to those that are displayed in Fig. 5; both diagonal elements approach $1/2$ in time scales determined by $t\propto 1/\sigma$, and the initial information regarding the value of the bit is lost.

Figure 6 shows the diffusion of the initial probability amplitudes in the full Hilbert space of 2^{16} coefficients for the numerical simulation of Fig. 5(c). Here starting from the initial two nonzero probability amplitudes, the state of the computer evolves to cover almost all of the Hilbert space by the time $\sigma t\sim 4$. Although some information about the initial

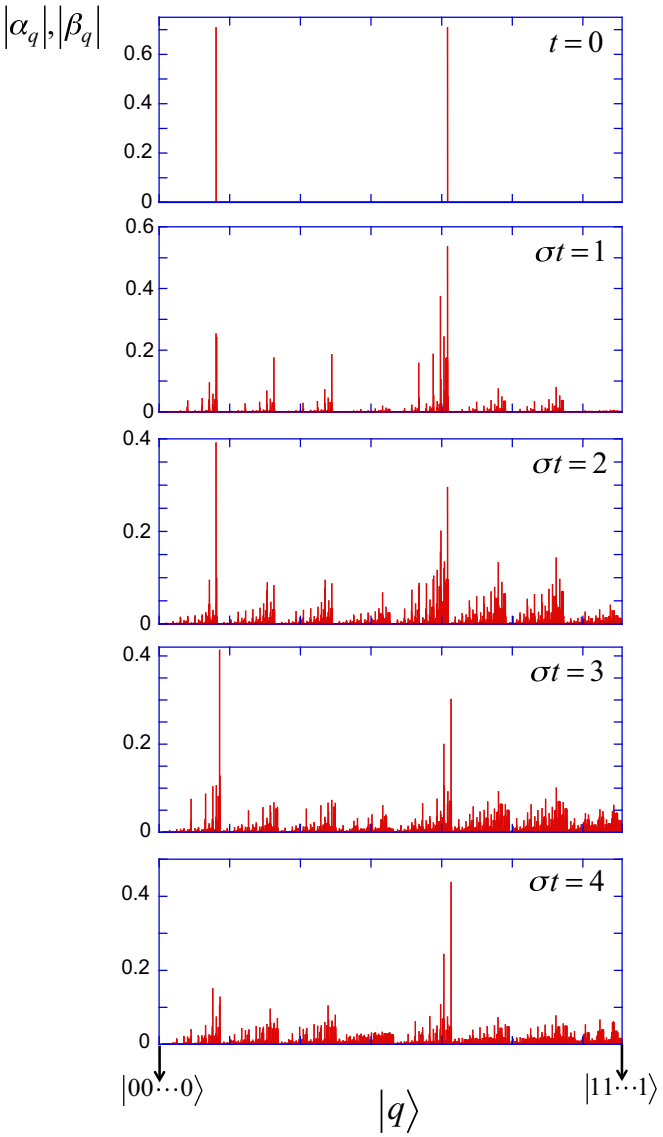

FIG. 6. The absolute value of the expansion coefficients at $t = 0$, $\sigma t = 1$, $\sigma t = 2$, $\sigma t = 3$, and $\sigma t = 4$ respectively. This simulation is performed for parameters that are identical to those used in the simulation of Fig. 5(c). Starting from the initial two nonzero probability amplitudes, the state of the computer evolves to cover almost all of the Hilbert space by the time $\sigma t \sim 4$.

condition remains by the time $\sigma t \sim 4$, the random nature of the leakage of the initial amplitudes to the Hilbert space is also clear even for this very small number of qubits.

In this section, we have shown that each qubit j in the computer decoheres in time scales $t \propto 1/\sigma$ due to correlated decay. As discussed in the introduction, if complexity classifications have a similar importance in quantum computation as in classical computation, then the fundamental result that the error always dominates for sufficiently large N is relevant regardless of the number N^* at which the error begins to dominate. However, there is no guarantee that $N \to \infty$ limit carries the same weight in quantum computing (as it does in classical computing), and we now have the tools to roughly estimate N^*. We stress that this is tangential to the main result, which is the mere existence of such an N^*. We define N^* through the condition $1/\sigma = t_0$, where σ is the width of the single-qubit Hamiltonian spectrum so that $1/\sigma$ is the time scale over which a single qubit decoheres, and t_0 is the gate time, which we take to have its smallest physically possible value, $t_0 = d/c$. As discussed above, $\sigma = \sqrt{NE'[F^2]/2}$, which leads to the condition $N^* = e^{\frac{2}{\pi}(c\kappa_a/\Gamma)^2}$ in 2D and $N^* = \frac{8}{(\pi+29/12)^3}(c\kappa_a/\Gamma)^6$ in 3D, respectively (we have averaged over all possible choices of single qubits j, so that $E'[F^2] \to E[F^2]$ where $E[\ldots]$ stands for the expected value over all possible pairs, and used the results of Appendix E for $E[F^2]$). For $N > N^*$, qubits decohere on time scales shorter than the gate time, making error correction impossible.

V. PHYSICAL DESCRIPTION OF THE SINGLE-QUBIT ERROR

The scaling of the single-qubit error with the total number of qubits in the computer can be understood using a qualitative classical argument which we discuss here. The key idea is that at the position of specific qubit j, the field emission from each of the other qubits interfere and cause this qubit to dephase. In the limit of $N \to \infty$, the radiation from other qubits at the position of qubit j has essentially random phases. As a result, the interference can be thought of as an incoherent sum of the radiated fields from the other qubits at the position of qubit j. Consider any other qubit in the computer, qubit k, at a distance $\vec{r}_{jk}$ away from qubit j. Classically qubit k can be viewed as a radiating dipole at the frequency of the qubit transition ω_a. This radiating dipole would then produce the following electric field at the position of qubit j [64]:

$$\mathcal{E}_{jk} = \frac{\eta\omega_a^2}{4\pi c}\frac{\mu}{r_{jk}}\exp(i\kappa_a r_{jk}). \tag{17}$$

Here, the quantity η is the impedance of free space $\eta = \sqrt{\mu_0/\epsilon_0}$, and μ is classically the strength of the radiating dipole (the dipole matrix element). In Eq. (17), for simplicity, we have ignored any angular dependence of the radiation pattern and considered the angular average. The electric field of Eq. (17) will interact with qubit j and cause unwanted rotation of the qubit states. The rate of this dephasing rotation is captured by the Rabi frequency due to the electric field:

$$\Omega_{jk} = \frac{\mu\mathcal{E}_{jk}}{\hbar} = \frac{\eta\omega_a^2}{4\pi\hbar c}\frac{\mu^2}{r_{jk}}\exp(i\kappa_a r_{jk}). \tag{18}$$

Equation (18) can be thought of as the dephasing rate of qubit j due to the presence of qubit k in the computer. Each qubit k in the computer produces an electric field given by Eq. (17). In the $N \to \infty$ limit, the quantities $\kappa_a r_{jk}$ become very large, and as a result, the radiated fields from individual qubits can be taken to have a random phase relationship with each other. The total electric field is then the incoherent sum from individual emissions $\mathcal{E}_{\text{total}} = \sqrt{\sum_k |\mathcal{E}_{jk}|^2}$ and the total dephasing rate is

$$\Omega_{\text{total}} = \sqrt{\sum_k |\Omega_{jk}|^2} = \left(\frac{3}{4}NE'[F^2]\right)^{1/2}. \tag{19}$$

This dephasing rate can be thought of as the single-qubit error rate. Note that this result agrees (within a prefactor) with

both of the results discussed in the previous section; i.e., the spread of the eigenvalue distribution σ of the single-qubit error Hamiltonian and the decay predicted by the analytical solution of Fig. 4.

VI. EIGENVALUE SPECTRUM OF THE TOTAL EXCHANGE HAMILTONIAN

We note that the previous sections have only considered approximate dynamics for estimating the single-qubit error on a given qubit by only including interactions in the exchange Hamiltonian $\hat{H}_{\text{eff}}$ which affect that qubit, i.e., the single-qubit error Hamiltonian $\hat{H}^j$. The width of the single-qubit Hamiltonian's spectrum gives the time scale over which state coefficients evolve if only those interactions are considered; in Sec. IV, we also showed that, as expected from the eigenvalue spectrum, the single-qubit coherence evolves on this time scale. However, because $[\hat{H}^{k_1k_2}, \hat{H}^{k_2k_3}] \neq 0$ for $k_1 \neq k_3$, this time evolution is approximate; although unlikely, there is the possibility that interactions between single-qubit Hamiltonians, the sum over which comprise the full exchange Hamiltonian, mitigate the errors. In this section, we show that this is not the case by finding the spectrum of the full Hamiltonian and showing that it is consistent with the picture in which each single-qubit Hamiltonian acts randomly and independently. Roughly speaking, if N single-qubit Hamiltonians act independently during each time step, changing the coefficient in a random direction but with magnitude typically σ (where σ is the width of the single-qubit error Hamiltonian spectrum), then the coefficient should change by typically $\sqrt{N}\sigma$ during that time step. If this holds for finite times, all moments of the exchange Hamiltonian spectrum should therefore be $\sqrt{N}$ times larger than the moments of the single-qubit error Hamiltonian, which is indeed the case. In this section, we will also discuss how error correction fails in another fundamental way. The width of the eigenvalue spectrum of the exchange Hamiltonian grows faster compared to the width of the system Hamiltonian. As a result, as $N \to \infty$, exchange interaction Hamiltonian dominates and can no longer be thought of as a perturbation to the system Hamiltonian. In fact, the system Hamiltonian becomes a perturbation on the exchange interaction Hamiltonian.

The eigenvalue distribution of the full exchange Hamiltonian $\hat{H}^{\text{eff}} = \sum_{(jk)} \hat{H}^{jk}$ can be found in the $N \to \infty$ and continuum limit by again finding the moments of the distribution, $\sigma^{(m)}$, for all integers m:

$$\begin{aligned}\sigma^{(m)} &= 2^{-N}\text{Tr}[(\hat{H}^{\text{eff}})^m] \\ &= 2^{-N}\sum_q \langle q|(\hat{H}^{\text{eff}})^m|q\rangle \\ &= 2^{-N}\sum_q \sum_{(k_1,l_1)} \cdots \sum_{(k_m,l_m)} \langle q|\hat{H}^{k_1l_1}\ldots\hat{H}^{k_ml_m}|q\rangle. \quad (20)\end{aligned}$$

This derivation is highly technical and the details are presented in Appendix D. The result is that the odd moments become negligible as $N \to \infty$, and the even moments fractionally converge to

$$\sigma^{(m)} \to m!\left(\tfrac{1}{2}NE[F^2]^{1/2}\right)^m. \quad (21)$$

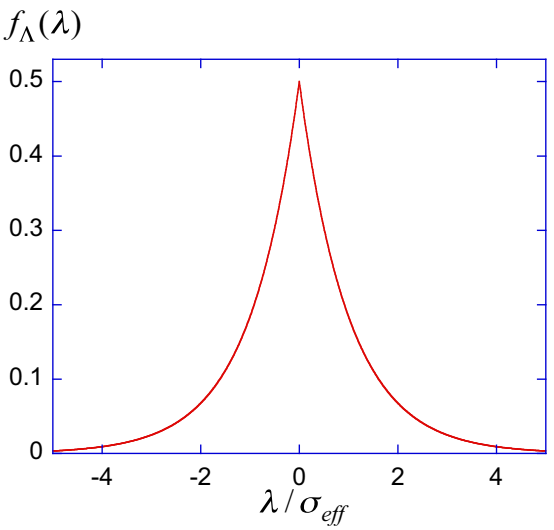

FIG. 7. The distribution of the eigenvalues of the total exchange Hamiltonian $\hat{H}_{\text{eff}}$ in the $N \to \infty$ limit. The eigenvalues are distributed according to the Laplace distribution, $f_\Lambda(\lambda) = \frac{1}{2\sigma_{\text{eff}}}\exp(-\frac{|\lambda|}{\sigma_{\text{eff}}})$ whose standard deviation is given by $\sigma_{\text{eff}} = \frac{1}{2}NE[F^2]^{1/2}$. The width of the spectrum scales as $\sigma_{\text{eff}} \sim N^{1/2}\ln N$ in 2D and $\sigma_{\text{eff}} \sim N^{2/3}$ in 3D respectively. Since in both geometries the spectrum spreads faster than the spectrum of the system Hamiltonian, $\frac{1}{2}\omega_a\sum_{j=1}^N \hat{\sigma}_z^j$, the dynamics of the computer become completely dominated by the noise due to correlated decay in the $N \to \infty$ limit.

Here, the notation $E[\ldots]$ refers to calculating the expected value of the quantity inside the brackets for all possible pairings of jk. Equation (21) shows that the eigenvalues of the full exchange Hamiltonian are distributed according to the Laplace distribution,

$$f_\Lambda(\lambda) = \frac{1}{2\sigma_{\text{eff}}}\exp\left(-\frac{|\lambda|}{\sigma_{\text{eff}}}\right), \quad (22)$$

whose standard deviation is given by $\sigma_{\text{eff}} = \frac{1}{2}NE[F^2]^{1/2}$. This distribution is plotted in Fig. 7. Using the scaling of the expected values of the coupling constants as discussed in Appendix E, the width of the spectrum scales as $\sigma_{\text{eff}} \sim N^{1/2}\ln N$ in 2D and $\sigma_{\text{eff}} \sim N^{2/3}$ in 3D respectively. Note that the computer system Hamiltonian without any noise is $\frac{1}{2}\omega_a\sum_{j=1}^N \hat{\sigma}_z^j$ (with possibly a gate Hamiltonian added on, which adds no N dependence). When $N \to \infty$, the eigenvalue distribution of the computer Hamiltonian thus becomes a Gaussian distribution, with standard deviation $\sigma_{\text{system}} = \omega_a\sqrt{N}/2$. Both in 2D and 3D geometry, the spectrum of the exchange interaction Hamiltonian has a spread that scales faster compared to the system Hamiltonian, showing that as $N \to \infty$ noise would dominate. To formalize this statement, for a Gaussian distribution, the odd moments are zero and the even moments are $(m-1)!!\sigma_{\text{system}}^m = (m-1)!!(\frac{1}{2}\omega_a N^{1/2})^m$ (the symbol "!!" stands for the double factorial). Thus the scaling of the mth moment (for m even) of the computer Hamiltonian is $N^{m/2}$, while for the exchange Hamiltonian it is $N^m E[F^2]^{m/2}$; in 2D $N^m E[F^2]^{m/2} \sim N^{m/2}\ln(N)^{m/2}$ and in 3D, $N^m E[F^2]^{m/2} \sim N^{m/2}N^{m/6}$. As a result, for both geometries for sufficiently large N the spectrum of the exchange Hamiltonian dominates over the computer Hamiltonian. When

the exchange interaction Hamiltonian dominates, the system can no longer be thought of as a collection of two-level systems. This is another way to see that the exchange Hamiltonian causes fundamental problems when considering scalability.

The eigenvalue spectrum of the full exchange Hamiltonian discussed above is consistent with each single-qubit error Hamiltonian decohering the quantum state randomly and independently. Suppose that there are no correlations between the single-qubit Hamiltonians $\hat{H}^j$, in the sense that for almost all states $|\psi\rangle$, the overlap between $\hat{H}^j|\psi\rangle$ and $\hat{H}^k|\psi\rangle$ for $j \neq k$ is approximately the overlap between two random states, which is the randomly signed sum of 2^N objects, each typically of the magnitude $(2^{-N/2})^2$, making the overlap typically $2^{-N/2}$. Then the norm of $\hat{H}_{\rm eff}|\psi\rangle$, which is typically $\sigma_{\rm eff}$, is $(\langle\psi|\hat{H}_{\rm eff}\hat{H}_{\rm eff}|\psi\rangle)^{1/2} = (\sum_{j,k}\langle\psi|\hat{H}^j\hat{H}^k|\psi\rangle)^{1/2}$. For $k = j$, $\langle\psi|(\hat{H}^j)^2|\psi\rangle$ is typically σ^2 in magnitude (σ is the width of the single-qubit error Hamiltonian). For $k \neq j$, $\langle\psi|\hat{H}^j\hat{H}^k|\psi\rangle$ is typically $\sigma^2 2^{-N/2}$ in magnitude under the assumption of no correlations between $\hat{H}^j, \hat{H}^k$. There are N terms with $k = j$ and N^2 with $k \neq j$, so for large N the $k \neq j$ terms don't matter and the norm of $\hat{H}_{\rm eff}|\psi\rangle$ is typically $\sqrt{N}\sigma$. Similar considerations show that the same relationship holds for all powers: The norm of $(\hat{H}_{\rm eff})^m|\psi\rangle$, which by definition is on average $\sigma^{(m)} \sim \sigma_{\rm eff}^m$, is typically $N^{m/2}\sigma_{\rm eff}$. As we have found, these are indeed the moments of the exchange Hamiltonian spectrum, which shows that the N single-qubit Hamiltonians do not have strong correlations between them, and therefore that the single-qubit Hamiltonian yields the correct time scale for the single-qubit error.

VII. CONCLUSIONS AND FUTURE DIRECTIONS

In conclusion, we have analyzed noise on quantum computers due to correlated decay between the qubit levels, which inevitably happens when the qubits are coupled to a common bosonic bath. We have first shown that even when the spacing between the qubits becomes larger than the emission wavelength, correlated decay produces errors outside the applicability of the threshold theorem. This is because the sum of the norms of the Hamiltonians (which can be viewed as the upper bound on the single-qubit error) that decoheres each qubit scales with the total number of qubits and is unbounded. We have then discussed two related results: (1) We have shown that for a majority of states in the Hilbert space, the actual error (instead of the upper bound) on each qubit scales with the number of qubits. As a result, in the limit of large number of qubits in the computer, $N \to \infty$, correlated decay causes each qubit in the computer to decohere in arbitrarily short time scales. (2) We have found the complete eigenvalue spectrum of the Hamiltonian that causes correlated decay in the same limit. We have shown that the spread of the eigenvalue distribution grows faster with N compared to the spectrum of the unperturbed system Hamiltonian. As a result, as $N \to \infty$, quantum evolution becomes completely dominated by the noise due to correlated decay.

One weakness of our results is that, throughout this paper, we have taken all the qubits to be causally connected to each other. It could perhaps be argued that if quantum error detection and correction cycle time is chosen to be sufficiently short, then before correlations causally reach all the qubits in the computer, errors can be corrected. We believe, however, that this argument is flawed. Suppose that we choose a fixed number of qubits, K, and during every quantum error correction cycle, we detect and correct errors on these K qubits. In this picture, we divide the full computer into clusters each of which contains K qubits. The error correction cycle is chosen to be sufficiently short such that K qubits in each cluster are causally connected to one another, but they are causally isolated from the rest of the computer. The main concern is that the qubits in each cluster can emit photons to the bath, which can propagate and at a later time be absorbed by another cluster. Unless the bosonic bath memory is erased, then bath correlations would propagate across the clusters and eventually cover the full computer (once sufficient time evolution is allowed so that the full computer is causally connected). To us, it is very hard to see how propagation of photons in the bath (causing "coupling" between clusters) can be avoided unless sections of the computer are completely isolated from one another. The physical picture that is developed in Sec. V is also helpful here. As noted above, this picture suggests that the radiated fields from all the other qubits in the computer interfere at the position of each qubit, causing decoherence that depends on the total number of qubits in the computer. In this picture, the precise emission time of the photons should not matter. The photons emitted from far-away points in the ensemble, even though they may have been emitted many quantum error correction cycles ago, would have similar strength and random phase as they reach a specific qubit in the ensemble. The scaling results that we discuss should, therefore, still be valid even though there may be many quantum error correction cycles during the time as the whole computer becomes causally connected.

In our view, our results put the scalability of quantum computers in 2D and 3D geometries into significant question, since any quantum system is inevitably coupled to a common bosonic bath. This being said, we certainly have not proven that noise due to correlated decay cannot be overcome. One strategy would be to use clever software (encoding) techniques of quantum information. It is now well understood that when the qubit-environment coupling is completely symmetric (small-sample regime), then quantum information can be protected from this kind of noise by encoding in decoherence free subspaces [43–45]. Unfortunately, such subspaces do not exist when the symmetries in the qubit-environment coupling are broken [46], which inevitably happens in the large sample case. But nevertheless, there are states with a reduced decoherence rate. For example, in the eigenvalue spectrum of the single-qubit error Hamiltonian of Fig. 2, there are eigenstates with an eigenvalue near zero. Because the standard deviation (the spread) of the whole distribution scales with the number of qubits, it is clear that the fraction of states with an eigenvalue smaller than a fixed threshold will be vanishingly small as $N \to \infty$. But perhaps it may be possible to show that scalable quantum computing can be performed in this vanishingly small fraction of the Hilbert space. We do note, however, that for complicated noise Hamiltonians (such as the exchange Hamiltonian that causes correlated decay) it is not clear how such special portions of

the Hilbert space can be calculated. For such systems, even calculating the ground state of the Hamiltonian is usually an exponentially-hard problem. This indicates that it is likely not possible to efficiently calculate the space of states with reduced decoherence properties for such complex Hamiltonians. As discussed in detail in Refs. [66,67], efficient calculation of the eigenstates of similar spin-glass Ising models would have far-reaching consequences in computational complexity.

Another strategy would be to design the computer at the hardware level to overcome correlated noise. A detailed discussion of various hardware strategies is left for a future publication, but we will mention a few ideas here. The key reason why correlated noise becomes uncorrectable is that every qubit interacts with and randomly decoheres every other qubit in the computer. It may be possible to physically isolate subsections of the computer so that they are uncoupled. Although it is not quite clear how this could be done, since subsections need to be entangled at some point during the computation and any entangling operation will necessarily include some kind of common environment coupling. Related to this idea, perhaps clusters of qubits at remote locations (coupled using, for example, long optical fibers) could be used. Yet another strategy would be to use a specific qubit system that would be less susceptible to correlated decay. Degenerate qubits (i.e., qubits with zero energy spacing between the qubit levels) and systems with varying qubit energies over the whole ensemble are known methods to reduce correlated decay. Our preliminary assessment of these strategies indicates that none of these ideas change the central results and the scalings in the problem; i.e., in the computational complexity terminology they modify the constants but not the N scalings. However, all of these ideas need to be carefully evaluated to clarify if the noise due to correlated decay can be overcome at a fundamental level.

We finally note that the exhange interaction is rather fundamental and is relevant in many interacting "spin" systems, ranging from polar molecules to Rydberg atoms [68]. Another future direction would be to explore the implications of the spectrum of the total exchange Hamiltonian of Fig. 7 in these other interacting spin systems.

ACKNOWLEDGMENTS

We thank Vickram Premakumar for his contributions at the early stages of this project and Josh Karpel for many helpful discussions. We also would like to thank an anonymous reviewer for in-depth criticism and useful comments that have allowed us to improve the paper significantly. This work was partially supported by startup funds from the University of Wisconsin–Madison, and the Wisconsin Alumni Research Foundation (WARF).

APPENDIX A: DERIVATION OF THE EXCHANGE HAMILTONIAN

In this Appendix, we discuss derivation of the effective exchange Hamiltonian of Eq. (3) starting with the total Hamiltonian for the system of Eq. (1) which describes the qubit ensemble, the bosonic bath, and the interaction between the two. This derivation follows steps that closely mimic the Wigner-Weiskoppf theory of spontaneous decay [63]. We take the the initial state of the qubit system to be an arbitrary (in general entangled) superposition state and assume that we start with zero photons in each field mode $\kappa\epsilon$. The initial state of the combined atom-radiation field system can be written as

$$|\psi(t=0)\rangle = \sum_{q=0}^{2^N-1} c_{q,0}|q\rangle \otimes |0\rangle. \tag{A1}$$

Here, the index q runs through all possible 2^N combinations for the qubits and c_q are the expansion coefficients. We define the following parameter for each atomic state $|q\rangle$:

$$2M_q \equiv \#\text{ of atoms in state}|1\rangle - \#\text{ of atoms in state}|0\rangle. \tag{A2}$$

With this definition, the energy of the atomic state $|q\rangle$ is $M_q\hbar\omega_a$. Working in the interaction picture, we expand the wave function as

$$\begin{aligned}|\psi(t)\rangle = &\sum_{q=0}^{2^N-1} c_{q,0}(t)\exp[-i(M_q\omega_a)t]\,|q\rangle \otimes |0\rangle \\ &+ \sum_{\kappa\epsilon}\sum_{q'=0}^{2^N-1} c_{q',1_{\kappa\epsilon}}(t) \\ &\times \exp[-i(M_{q'}\omega_a + \nu_{\kappa\epsilon})t]\,|q'\rangle \otimes |1_{\kappa\epsilon}\rangle. \end{aligned}\tag{A3}$$

Here, $|1_{\kappa\epsilon}\rangle$ represents the state of the radiation field in which the field mode $\kappa\epsilon$ has one photon while all the other modes are in vacuum state and the quantity $\nu_{\kappa\epsilon}$ is the frequency of this mode. With these definitions, the Schrödinger's equation

$$i\hbar\frac{d|\psi(t)\rangle}{dt} = \hat{H}_{\text{total}}|\psi(t)\rangle \tag{A4}$$

yields the following continuum of coupled equations:

$$\begin{aligned}\frac{dc_{q,0}}{dt} &= i\sum_{\kappa\epsilon} g_{\kappa\epsilon}\sum_j \exp(i\vec{\kappa}\cdot\vec{r}_j)c_{q\ominus j,1_{\kappa\epsilon}}(t) \\ &\quad\times \exp[-i(\nu_{\kappa\epsilon}-\omega_a)t], \\ \frac{dc_{q\ominus j,1_{k\epsilon}}}{dt} &= ig_{\kappa\epsilon}\sum_k \exp(-i\vec{\kappa}\cdot\vec{r}_k)c_{q\ominus j\oplus k,0}(t) \\ &\quad\times \exp[-i(\omega_a-\nu_{\kappa\epsilon})t]. \end{aligned}\tag{A5}$$

Here, as mentioned in the main text, we use the notation $|q\ominus j\rangle$ to mean the configuration that equals $|q\rangle$ at all qubits except the qubit j which has undergone a $|1\rangle^j \to |0\rangle^j$ transition. The quantity $\vec{r}_j$ is the position vector of the qubit j. Similarly, the configuration $|q\ominus j\oplus k\rangle$ differs from $|q\ominus j\rangle$ by raising qubit k (at the position $\vec{r}_k$) from $|0\rangle^k \to |1\rangle^k$. The coupled equations of above are intuitive. Each specific configuration $|q\rangle$ is coupled to configurations where a qubit is lowered (configurations $|q\ominus j\rangle$) by emitting a photon into the bath. Similarly, each configuration $|q\ominus j\rangle$ is coupled to configurations where a qubit is raised (configurations $|q\ominus j\oplus k\rangle$) by absorbing a photon from the bath. We then formally integrate the equations that contain bath excitations

$c_{q\ominus j,1_{\kappa\epsilon}}$

$$c_{q\ominus j,1_{\kappa\epsilon}}(t) = ig_{\kappa\epsilon}\sum_k \exp(-i\vec{\kappa}\cdot\vec{r}_k) \times \int_0^t \exp[-i(\omega_a - \nu_{\kappa\epsilon})t']c_{q\ominus j\oplus k,0}(t')dt'. \tag{A6}$$

Here, it is assumed that the coupling to the radiation modes is turned on at $t = 0$. It is also assumed that the initial conditions for the continuum mode amplitudes are $c_{q\ominus j,1_{\kappa\epsilon}}(t = 0) = 0$. Using Eq. (A6), the differential equation for $c_{q,0}$ in Eq. (A5) now reads

$$\frac{dc_{q,0}}{dt} = -\sum_{\kappa\epsilon}|g_{\kappa\epsilon}|^2\sum_j\sum_k \exp(i\vec{\kappa}\cdot\vec{r}_{jk}) \times \int_0^t \exp[-i(\nu_{\kappa\epsilon} - \omega_a)(t - t')]c_{q\ominus j\oplus k,0}(t')dt', \tag{A7}$$

where we have defined $\vec{r}_{jk} \equiv \vec{r}_j - \vec{r}_k$. This way, the problem is reduced to a set of coupled integrodifferential equations for the initial probability amplitudes $c_{q,0}$. Each state $|q\rangle$ is coupled to all states that differ by lowering one qubit and raising another qubit in the configuration (i.e., to states $|q \ominus j \oplus k\rangle$). We next rewrite the summation as an integral since we are considering a continuum of radiation modes:

$$\sum_{\kappa\epsilon}|g_{\kappa\epsilon}|^2 \to \frac{V}{(2\pi)^3}\int_{\kappa\epsilon}|g_{\kappa\epsilon}|^2 d^3\kappa. \tag{A8}$$

Here, $\kappa = |\vec{\kappa}|$ and V is the quantization volume which is assumed to be much larger than the qubit ensemble. We proceed in spherical coordinates and replace $d^3\kappa$ integral with $d^3\kappa = \kappa^2\sin\theta d\kappa d\theta d\phi$. The coupling constants $g_{\kappa\epsilon}$ depend on the matrix element between the two levels and also the angle between the polarization of a particular electromagnetic mode and the orientation of the atomic dipole:

$$|g_{\kappa\epsilon}|^2 = \frac{\nu_{\kappa\epsilon}\mu^2}{2\epsilon_0\hbar V}(\vec{\epsilon}\cdot\vec{\epsilon}_a)^2. \tag{A9}$$

Here, μ is the coupling matrix element between the two levels (electric-dipole or magnetic-dipole), $\vec{\epsilon}$ is the polarization vector of the mode with frequency $\nu_{k\epsilon}$, and $\vec{\epsilon}_a$ is the orientation vector of the atomic dipole. With these definitions, Eq. (A7) reads

$$\frac{dc_{q,0}}{dt} = -\frac{\mu^2}{2(2\pi)^3\epsilon_0\hbar c^3}\sum_j\sum_k\int_0^\infty \nu_\kappa^3 \times\left[\int_0^\pi\int_0^{2\pi}\sin\theta(\vec{\epsilon}\cdot\vec{\epsilon}_a)^2\exp(i\vec{\kappa}\cdot\vec{r}_{jk})d\theta d\phi\right] \times\left[\int_0^t \exp[-i(\nu_\kappa - \omega_a)(t - t')]c_{q\ominus j\oplus k,0}(t')dt'\right]d\nu_\kappa. \tag{A10}$$

Here, we have used the identity $\kappa = \nu_\kappa/c$ to convert the outermost integral from $d\kappa$ to $d\nu_\kappa$. The middle angular integral can be evaluated analytically:

$$\int_0^\pi\int_0^{2\pi}\sin\theta(\vec{\epsilon}\cdot\vec{\epsilon}_a)^2\exp(i\vec{\kappa}\cdot\vec{r}_{jk})d\theta d\phi = 4\pi(1-\cos^2\theta_{jk})\frac{\sin(\kappa r_{jk})}{\kappa r_{jk}} + 4\pi(1-3\cos^2\theta_{jk}) \times\left[\frac{\cos(\kappa r_{jk})}{(\kappa r_{jk})^2} - \frac{\sin(\kappa r_{jk})}{(\kappa r_{jk})^3}\right]. \tag{A11}$$

Here $r_{jk} = |\vec{r}_{jk}|$ and the angle θ_{jk} is the angle between the atomic dipole moment vector $\vec{\epsilon}_a$ and the separation vector $\vec{r}_{jk}$:

$$\cos\theta_{jk} = \frac{(\vec{\epsilon}_a\cdot\vec{r}_{jk})^2}{r_{jk}^2}. \tag{A12}$$

To evaluate the time and frequency integrals in Eq. (A10), we employ the usual Born-Markov approximation. For this purpose we replace $c_{q\ominus j\oplus k,0}(t')$ with $c_{q\ominus j\oplus k,0}(t)$ and take this quantity outside the integral. We also consider the $t \to \infty$ limit of the inner time integral, which results in $\int_0^\infty \exp[i(\nu_\kappa - \omega_a)t']dt' = \pi\delta(\nu_\kappa - \omega_a) + i\mathrm{P}\{\frac{1}{\nu_\kappa - \omega_a}\}$ (δ is the Dirac δ function and P{} stands for the principal value). Using all of these results and simplifications, Eq. (A10) reduces to

$$\frac{dc_{q,0}}{dt} = -\sum_j\sum_k F_{jk}c_{q\ominus j\oplus k,0}, \tag{A13}$$

where F_{jk} are the exchange coupling coefficients as defined in Eq. (5).

1. Beyond the Born-Markov approximation

The Born-Markov approximation that allows the derivation of the effective exchange Hamiltonian of Eq. (3) assumes the evolution time scales for the state coefficients to be slow compared to the correlation time scales of the bath. It is important to understand our system beyond this approximation, since as $N \to \infty$ the system dynamics become ever faster and Born-Markov approximation is violated. We recently developed a model of correlated decay that goes beyond the Born-Markov approximation and models finite time scales of bath correlations and propagation effects across the sample. We will discuss the details of this model, including its derivation, in a future publication. Briefly, in this model, the state coefficients evolve according to an integrodifferential equation of the form

$$\frac{dc_q}{dt} = -\left(\frac{3}{8\pi}\right)\frac{\Gamma}{2}\sum_j\sum_k(1-\cos^2\theta_{jk})\int_0^t \exp[i\omega_a(t-\tau)] \times G(t-\tau)c_{q\ominus j\oplus k}(\tau)d\tau, \tag{A14}$$

where

$$G(t-\tau) \equiv \frac{2\pi}{(r_{jk}/c)}\mathrm{Box}\left[\frac{t-\tau}{(r_{jk}/c)}\right] - i\frac{2}{(r_{jk}/c)}\ln\left[\frac{(r_{jk}/c)+(t-\tau)}{|(r_{jk}/c)-(t-\tau)|}\right]. \tag{A15}$$

Here, the Box function equals one when its argument is between 0 and 1, and equals zero otherwise. The integration kernel $G(t-\tau)$ captures the correlation (memory) time scales

of the bath, which has a width of order r_{jk}/c. We have verified that the above model is consistent with many other formulations of large-sample super-radiance, as discussed in detail, for example, in the review article Ref. [48], Sec. 7. The above model clarifies the effect of the Born-Markov approximation in large samples. If the evolution time scales for the state coefficients are slow compared to the width of the function $G(t-\tau)$, then the kernel effectively acts like a δ function. Under these conditions, $c_{q\ominus j\oplus k}(\tau)$ coefficients can be taken outside the integral and be replaced by $c_{q\ominus j\oplus k}(\tau) \approx c_{q\ominus j\oplus k}(t)$. If the coefficients are not slowly varying, then this approximation cannot be applied. When the Born-Markov approximation is not satisfied, the rate of change in each coefficient c_q is not only influenced by the values of the coefficients at that particular time, $c_{q\ominus j\oplus k}(t)$, but instead depends the values of the coefficients over the time window $[t,t-r_{jk}/c]$. We note that all the scaling results that we discuss in the paper result from N-dependent sums over the prefactors in fronts of these coefficients, which have almost random phases (due to large spacings) and $1/r_{jk}$ scaling factors. It is very hard to see how any of these scaling results could be altered when one considers not just the values of the coefficients at that particular time but also takes into account their evolution history, since neither phases nor the average strengths of the prefactors are altered.

As discussed in Sec. V above, a good physical model for correlated decay in large samples can be summarized as follows: Consider a specific qubit j in the ensemble. The radiated fields from all the other qubits in the computer interfere at the position of the qubit j producing a randomly fluctuating field. This fluctuating field results in random phase rotations and population transfer in qubit j, causing bit-flip and decoherence errors. When the Born-Markov approximation is satisfied, we evaluate the field values at a specific point in time and consider their interference. When the Born-Markov approximation is violated, we need to take into account not only each emitted field at a specific point in time, but also the history of the field over the window $[t,t-r_{jk}/c]$. But for both cases, neither the number of fields that are interfering nor the average strength of each field is altered. As a result, the scaling results that we discuss should remain valid even when the Born-Markov approximation is violated.

APPENDIX B: THE EIGENVALUE SPECTRUM OF THE SINGLE-QUBIT ERROR HAMILTONIAN

Here we present the details of deriving the eigenvalue distribution of the single-qubit error Hamiltonian $\hat{H}^j$ in the limit of $N\to\infty$. The method outlined below is more complicated than it needs to be, but it introduces the ideas and definitions necessary for the case of the full exchange Hamiltonian $\hat{H}_{\rm eff}$, which is discussed in Appendix D. The distribution of the eigenvalues can be reconstructed by evaluating the moments, the mth of which is defined as

$$\sigma^{(m)} = 2^{-N}\mathrm{Tr}[(\hat{H}^j)^m]. \tag{B1}$$

To compute the trace, we use the basis of states $|q\rangle$ which correspond to definite arrangements q of the qubits. For example, with $N=6$, one q is $\{\{1,1\},\{2,0\},\{3,0\},\{4,1\},\{5,1\},\{6,0\}\}$, which indicates that the first qubit is raised, the second is lowered, the third is lowered, and so forth. Let the space of arrangements of any set of qubits $\mathcal{Q}$ be $\mathcal{A}_\mathcal{Q}$; defining $\mathcal{N}$ be the set of all qubits, $q\in\mathcal{A}_\mathcal{N}$. We will make use of the space $\mathcal{A}_\mathcal{Q}$ for $\mathcal{Q}\neq\mathcal{N}$, which makes the explicit reference to the qubit labels in the arrangements q useful. Note that the common convention in which the qubit label is deduced from the location, i.e., $\{\{1,1\},\{2,0\},\{3,0\},\{4,1\},\{5,1\},\{6,0\}\}\to\{100110\}$, is more concise but is only unambiguous when dealing with arrangements of all qubits, i.e., $\mathcal{Q}=\mathcal{N}$. To make the distinction between these cases clear, we reserve the letter q for elements of $\mathcal{A}_\mathcal{N}$, and use r for elements of $\mathcal{A}_\mathcal{Q}$ when $\mathcal{Q}\subset\mathcal{N}$. Thus above, $q\in\mathcal{A}_\mathcal{N}$, but $r=\{\{1,1\},\{4,0\}\}\in\mathcal{A}_{\{1,4\}}$.

Each of the N qubits can be 0 or 1, which we call "lowered" and "raised" respectively, so $2^N=|\mathcal{A}_\mathcal{N}|$ is the number of elements in $\mathcal{A}_\mathcal{N}$. Expressing the trace in this basis results in

$$\sigma^{(m)} = 2^{-N}\sum_{q\in\mathcal{A}_\mathcal{N}}\langle q|(\hat{H}^j)^m|q\rangle. \tag{B2}$$

First we expand each of the m Hamiltonians as a sum of pair Hamiltonians $\hat{H}^j=\sum_{k\neq j}\hat{H}^{jk}$ and then expand the product over the m Hamiltonians:

$$\sigma^{(m)} = 2^{-N}\sum_{q\in\mathcal{A}_\mathcal{N}}\langle q|\sum_{k_1}\sum_{k_2}\cdots\sum_{k_m}\hat{H}^{jk_1}\hat{H}^{jk_2}\ldots\hat{H}^{jk_m}|q\rangle, \tag{B3}$$

where the restriction that each sum is over qubits $k_\alpha\neq j$ is implicit, in order to avoid the notation becoming too cumbersome.

For each ordered sequence of m qubits $\{k_1\ldots k_m\}$, given a state $|q\rangle$, it is either the case that $\langle q|\hat{H}^{jk_1}\ldots\hat{H}^{jk_m}|q\rangle = F_{jk_1}\ldots F_{jk_m}$, in which case we call this sequence compatible with q, or else $\langle q|\hat{H}^{jk_1}\ldots\hat{H}^{jk_m}|q\rangle=0$, in which case we call this sequence incompatible with q. Let $\mathcal{K}^m_\mathcal{Q}$ be the set of all ordered sequences of m qubits chosen from the set $\mathcal{Q}$, and introduce a function $\omega(q,K)$, which accepts an arrangement in $q\in\mathcal{A}_\mathcal{N}$ and a sequence $K\in\mathcal{K}^m_\mathcal{Q}$, and returns 1 if they are compatible and 0 if they are incompatible. Defining $\prod F(K)\equiv\prod_{\alpha=1}^m F_{jk_\alpha}$ for $K=\{k_1\ldots k_m\}$ and denoting the set of all qubits besides j as $\mathcal{N}'$,

$$\begin{aligned}\sigma^{(m)} &= 2^{-N}\sum_{q\in\mathcal{A}_\mathcal{N}}\sum_{k_1}\cdots\sum_{k_m}\prod F(\{k_1\ldots k_m\})\omega(q,\{k_1\ldots k_m\})\\ &= 2^{-N}\sum_{q\in\mathcal{A}_\mathcal{N}}\sum_{K\in\mathcal{K}^m_{\mathcal{N}'}}\prod F(K)\omega(q,K)\\ &= 2^{-N}\sum_{K\in\mathcal{K}^m_{\mathcal{N}'}}\prod F(K)\sum_{q\in\mathcal{A}_\mathcal{N}}\omega(q,K).\end{aligned} \tag{B4}$$

Let us divide the set $\mathcal{K}^m_\mathcal{Q}$ into subsets in which each element (sequence) of the subset has the same number of unique qubits. We will denote the space of all sequences of m qubits chosen from the set $\mathcal{Q}$ with u unique qubits appearing in it by $\mathcal{K}^m_\mathcal{Q}(u)$. $\mathcal{K}^m_\mathcal{Q}=\mathcal{K}^m_\mathcal{Q}(1)\cup\mathcal{K}^m_\mathcal{Q}(2)\cup\cdots\cup\mathcal{K}^m_\mathcal{Q}(m\wedge|\mathcal{Q}|)$ and $\mathcal{K}^m_\mathcal{Q}(u_1)\cap\mathcal{K}^m_\mathcal{Q}(u_2)=0$ for $u_1\neq u_2$ (we use the notation $a\wedge b$ to mean the smaller of a,b), so we may express the sum over

K as

$$\sigma^{(m)} = 2^{-N} \sum_{u=1}^{m\wedge|\mathcal{N}'|} \sum_{K\in\mathcal{K}^m_{\mathcal{N}'}(u)} \prod F(K) \sum_{q\in\mathcal{A}_{\mathcal{N}}} \omega(q,K). \quad \text{(B5)}$$

We only require $\sigma^{(m)}$ out to arbitrarily high but finite order, so we take $m \wedge |\mathcal{N}'| = m \wedge (N-1) = m$.

We note that $\omega(q,\{k_1 \ldots k_m\}) = 1$ if and only if $|q\rangle = \hat{H}^{k_1 j} \ldots \hat{H}^{k_m j}|q\rangle$. Thus for m odd, there are no sequences compatible with any states, and so $\sigma^{(m)} = 0$; from now on we focus exclusively on the case that m is even. Because the product $\hat{H}^{jk_1} \ldots \hat{H}^{jk_m}$ only acts nontrivially on j and the qubits which appear in the sequence $\{k_1 \ldots k_m\}$, all arrangements which agree on these qubits will be compatible or incompatible with the same sequences. To formalize this statement, let $\mathcal{U}_K$ be the unordered set of u unique qubits which appear in the sequence $K \in \mathcal{K}^m_{\mathcal{Q}}(u)$. Then for any $K \in \mathcal{K}^m_{\mathcal{Q}}(u)$, for any $r \in \mathcal{A}_{\mathcal{U}_K\cup\{j\}}$, and for all $q,q' \in \mathcal{A}_{\mathcal{N}}$ and $q,q' \supseteq r$, $\omega(q,K) = \omega(q',K)$. Thus we may unambiguously define a new function $\tilde{\omega}(r \in \mathcal{A}_{\mathcal{U}_K\cup\{j\}}, K \in \mathcal{K}^m_{\mathcal{Q}}(u))$, which accepts a sequence and arrangements of j and the qubits appearing in that sequence (as opposed to ω which accepts a sequence and arrangements of all N qubits), to be equal to $\omega(q,K)$ for any $q \supseteq r$, $q \in \mathcal{A}_{\mathcal{N}}$. For example, consider a four-qubit computer with $\mathcal{N} = \{1,2,3,4\}$, and focus on pair Hamiltonian sequences $K \in \mathcal{K}^2_{\{1,4\}}$ that only involve qubits 1 and 4. Then if we consider all arrangements q where qubit 1 is lowered and qubit 4 is raised, $r = \{\{10\},\{41\}\} \in \mathcal{A}_{\{1,4\}}$, the states of qubits 2 and 3 are irrelevant for compatibility, i.e., $\omega(\{10\},\{20\},\{30\},\{41\}),K) = \omega(\{\{10\},\{21\},\{30\},\{41\}\},K) = \omega(\{\{10\},\{20\},\{31\},\{41\}\},K) = \omega(\{\{10\},\{21\},\{31\},\{41\}\},K) = \tilde{\omega}(\{\{10\},\{41\}\},K)$.

For each sequence $K \in \mathcal{K}^m_{\mathcal{Q}}(u)$, for any $r \in \mathcal{A}_{\mathcal{U}_K\cup\{j\}}$, there are 2^{N-u-1} unique $q \in \mathcal{A}_{\mathcal{N}}$ that contain q, because each of the $N-u-1$ qubits which are not j or in $\mathcal{U}_K$ can be up or down for such a q. Therefore, $\sum_{q\in\mathcal{A}_{\mathcal{N}}} \omega(q, K \in \mathcal{K}^m_{\mathcal{N}'}(u)) = 2^{N-u-1} \sum_{r\in\mathcal{A}_{\mathcal{U}_K\cup\{j\}}} \tilde{\omega}(r,K)$, which allows us to write

$$\sigma^{(m)} = \sum_{u=1}^{m} 2^{-u-1} \sum_{K\in\mathcal{K}^m_{\mathcal{N}'}(u)} \prod F(K) \sum_{r\in\mathcal{A}_{\mathcal{U}_K\cup\{j\}}} \tilde{\omega}(r,K). \quad \text{(B6)}$$

To calculate Eq. (B6), we wish to isolate the N dependence of the different pieces of this sum, so that we may keep only the important parts as $N \to \infty$. To this end, note that we can construct any sequence $\{k_1 \ldots k_m\} = K \in \mathcal{K}^m_{\mathcal{Q}}(u)$ out of (1) an ordered list of u subsets of the first m integers and (2) an ordered list of u unique qubits which are not j. The sequence is then constructed by assigning the first location in the sequence the integer 1, the second location the integer 2, etc., and then placing the first qubit in the qubit list at all locations in the sequence associated with the integers contained in the first subset, the second qubit at all locations associated with integers in the second subset, and so forth until the uth qubit has been assigned. For example, the sequence $\{2,5,14,2,2,5,2,14\}$ with $m = 8$ and $u = 3$ is constructed by the integer subsets $\{\{145\},\{26\},\{38\}\}$ and the qubit list $\{2,5,14\}$. A set of integer subsets paired with a qubit list generates a sequence as long as there are the same number of subsets as qubits, and each integer appears in exactly one subset. We will call a set of integer subsets in which each integer appears in exactly one subset a pattern (we do not employ the notion of a partition because it does not extend to the full Hamiltonian case) and denote the set of all patterns of m integers with u subsets by $\mathcal{S}_m(u)$, so that the set of all patterns of m integers is $\mathcal{S}_m = \mathcal{S}_m(1) \cup \mathcal{S}_m(2) \cup \cdots \cup \mathcal{S}_m(m)$. We will call $\mathcal{L}^u_{\mathcal{Q}}$ the set of all ordered lists of u unique qubits chosen from the set of qubits $\mathcal{Q}$. We define a function S to take a pattern and a qubit list, and return the constructed sequence, i.e., if $K \in \mathcal{K}^m_{\mathcal{Q}}(u)$ is the sequence constructed by $s \in \mathcal{S}_m(u)$ and $L \in \mathcal{L}^u_{\mathcal{Q}}$, then $S(s,L) = K$. Then, because every sequence can be constructed by some pattern and qubit list, we may express the moments as

$$\sigma^{(m)} = \sum_{u=1}^{m} 2^{-u-1} \sum_{s\in\mathcal{S}_m(u)} \sum_{L\in\mathcal{L}^u_{\mathcal{N}'}} \frac{1}{\Lambda(S(s,L))} \prod F(S(s,L)) \times \sum_{r\in\mathcal{A}_{\mathcal{U}_{S(s,L)}\cup\{j\}}} \tilde{\omega}(r,S(s,L)), \quad \text{(B7)}$$

where $\Lambda(K)$ is the number of combinations of patterns and qubit lists such which, when given as the argument of S, yield $S = K$. Each pattern and qubit list is associated with one sequence, but each sequence is associated with many pattern and qubit list combinations, so we must divide the degeneracy factor Λ to prevent overcounting. All sequences are paired uniquely with a set of subsets which make up a pattern; this is done by writing down subsets containing the integer locations of each qubit. The order is left arbitrary, and the sequence $K(s,L)$ will not be altered if we reorder the subsets in s and then reorder the qubits in L in the same way. Thus, $\Lambda(s) = u!$ for $s \in \mathcal{S}_m(u)$.

The system is invariant under the relabelling of qubits, so it must be that the quantity $\sum_{q\in\mathcal{A}_{\mathcal{U}_{S(s,L)}\cup\{j\}}} \tilde{\omega}(q,S(s,L)) \equiv \Omega(s)$ does not depend on the choice of qubits. This allows us to write

$$\sigma^{(m)} = \sum_{u=1}^{m} \frac{1}{2^{u+1}u!} \sum_{s\in\mathcal{S}_m(u)} \Omega(s) \sum_{L\in\mathcal{L}^u_{\mathcal{N}'}} \prod F(S(s,L)). \quad \text{(B8)}$$

There is no N dependence in $|\mathcal{S}_m(u)|$ or $\Omega(s)$. Thus for fixed m, the above sum is a fixed number of terms (one for each pattern $s \in \mathcal{S}_m$), with a fixed coefficient (equal to $\Omega(s)/2^{u+1}u!$) in front of an N-dependent sum $\sum_{L\in\mathcal{L}^u_{\mathcal{N}'}} \prod F(S(s,L)) \equiv G_s(N)$:

$$\sigma^{(m)} = \sum_{u=1}^{m} \frac{1}{2^{u+1}u!} \sum_{s\in\mathcal{S}_m(u)} \Omega(s) G_s(N). \quad \text{(B9)}$$

We now examine the scaling with large N of the sums $\sum_{L\in\mathcal{L}^u_{\mathcal{N}'}} \prod F(S(s,L)) = G_s(N)$ for patterns with nonzero coefficients, i.e., $\Omega(s) \neq 0$, and keep only the patterns for which the N scaling is the largest among these, creating a new quantity which will fractionally converge to $\sigma^{(m)}$ in the high-N limit. We use the notation $A \to B$ to mean that A fractionally converges to B, i.e., $A/B = 1$ in the limit that N goes to infinity.

We note that $\mathcal{L}^u_{\mathcal{N}'}$ is the set of all ways to make an ordered list of u unique qubits chosen from the set of all qubits except j, so $|\mathcal{L}^u_{\mathcal{N}'}| = \binom{N-1}{u} u! \to N^u$ is the number of ways to pick u qubits times the number of ways to order them. Thus, by the

definition of the expectation value of a pattern, $E'_s[\prod F]$, as defined in Appendix F, we have

$$G_s(N) = \sum_{L\in\mathcal{L}^u_{\mathcal{N}'}} \prod F(S(s,L)) = \frac{(N-1)!}{(N-1-u)!} E'_s\Big[\prod F\Big] \to N^u E'_s\Big[\prod F\Big]. \tag{B10}$$

In order for $\Omega(s)\neq 0$, each of the u subsets in the pattern s must contain some even number of integers. Let p_z be the number of integers in the zth subset; then $\sum_{z=1}^{u} p_z = m$, all p_z are even, each $p_z \geqslant 2$, and for any set of integers $\{p_1,\ldots,p_u\}$ which obey these conditions, there is some pattern s for which $\Omega(s)\neq 0$ and with p_z integers in its zth subset. For a pattern s with at least one $p_z > 2$, we compare the N scaling of $G(s,N)$ to the scaling of $G(s',N)$, where s' is the same as s except that one of the p_z greater than 2 has been reduced by 2, and u has been increased by 1, adding a $p_{u+1} = 2$; i.e., if s has $\{p_1,\ldots,p_i,\ldots p_u\}$ where $p_i > 2$, then s' has $\{p_1,\ldots,p_i-2,\ldots p_u,2\}$. As shown in Appendix F, $E'_s(\prod F) <_N N E'_{s'}[\prod F]$ (where $<_N$ means "has smaller N scaling than"), so

$$G_s(N) \to N^u E'_s\Big[\prod F\Big] <_N N^{u+1} E'_{s'}\Big[\prod F\Big] = G_{s'}(N), \tag{B11}$$

and we conclude that terms corresponding to the pattern s becomes negligible compared to s' in the high-N limit (as long as $\Omega(s')\neq 0$, which is true if $\Omega(s)\neq 0$). This transformation may be repeatedly applied to all patterns for which some $p_z \neq 2$, and thus all such patterns may be ignored in favor of patterns for which all $p_z = 2$. Keeping only these, which are all of the patterns with $u = m/2$,

$$\sigma^{(m)} \to \frac{1}{2^{m/2+1}(m/2)!}\sum_{s\in\mathcal{S}_m(m/2)} \Omega(s) G_s(N) \to \frac{1}{2^{m/2+1}(m/2)!}\sum_{s\in\mathcal{S}_m(m/2)} \Omega(s) N^{m/2} E'_s\Big[\prod F\Big]. \tag{B12}$$

Recall that $\Omega(s) = \sum_{q\in\mathcal{A}_{\mathcal{U}_{S(s,L)}\cup\{j\}}} \tilde{\omega}(q,S(s,L))$, for $s\in\mathcal{S}_m(m/2)$; in order for $\tilde{\omega}(q,S(s,L))$ to be nonzero the qubits in $\mathcal{U}^{m/2}_{S(s,L)}$ must have the 'correct' relative status to j in q, depending on the locations they appear at in the sequence. For example, suppose j is raised in q; if $\langle q|\hat{H}_{jk_1}\hat{H}_{jk_2}\hat{H}_{jk_2}\hat{H}_{jk_1}|q\rangle \neq 0$, then k_1 must be lowered in q, and k_2 must be raised. Thus $\Omega(s\in\mathcal{S}_m(m/2)) = 2$, corresponding to the two possibilities for qubit j, which yields

$$\sigma^{(m)} \to \frac{N^{m/2}}{2^{m/2+1}(m/2)!}\sum_{s\in\mathcal{S}_m(m/2)} 2E'_s\Big[\prod F\Big] = \frac{N^{m/2}}{2^{m/2}(m/2)!}\sum_{s\in\mathcal{S}_m(m/2)} E'_s\Big[\prod F\Big]. \tag{B13}$$

The expectation value of $\prod F$, which is $\sum_{(k_1\ldots k_{m/2})} F^2_{jk_1}\ldots F^2_{jk_{m/2}}/\binom{N}{m/2}$, is the same for all patterns in $\mathcal{S}_m(m/2)$; we denote this by $E'_{(2,m)}[\prod F]$, and utilize the fact that there is no longer any s dependence in the summand to write

$$\sigma^{(m)} \to \frac{N^{m/2}}{2^{m/2}(m/2)!}\sum_{s\in\mathcal{S}_m(m/2)} E'_{(2,m)}\Big[\prod F\Big] = \frac{N^{m/2}}{2^{m/2}(m/2)!} E'_{(2,m)}\Big[\prod F\Big]|\mathcal{S}_m(m/2)|. \tag{B14}$$

The patterns in $\mathcal{S}_m(m/2)$ are all of the ways to pair up the integers, but because the status of j alternates after each Hamiltonian is applied, each odd integer must be paired with an even integer. We may order these $m/2$ pairs in any way, so $|\mathcal{S}_m(m/2)| = (m/2)!\times(m/2)!$. Using the result in Appendix F that $E'_{(2,m)}[\prod F] \to E'[F^2]^{m/2}$ (where $E'[F^2] \to N^{-1}\sum_{k\neq j} F^2_{jk}$), we finally obtain

$$\begin{aligned} \sigma^{(m)} &\to (m/2)!(N E'[F^2]/2)^{m/2}, && m \text{ even},\\ \sigma^{(m)} &= 0, && m \text{ odd}. \end{aligned} \tag{B15}$$

APPENDIX C: DYNAMICS OF THE REDUCED DENSITY MATRIX FOR A SPECIFIC QUBIT

In this Appendix, we discuss the details of the Taylor-series analytical solution of Eq. (B14), which is plotted in Fig. 4. Consider the initial condition that only one of the α_Q coefficients for a specific configuration Q is nonzero, $\alpha_Q(t=0)=1;\alpha_q(t=0)=0$ for $q\neq Q;\beta_q(t=0)=0$. We view this initial condition as the zeroth-order solution: $\alpha^{(0)}_Q = 1;\alpha^{(0)}_q = 0$ for $q\neq Q;\beta^{(0)}_q = 0$. To find the first-order solutions, we solve the coupled equations of Eqs. (13) using the zeroth-order solution on the right-hand side of the equations:

$$i\frac{d\alpha^{(1)}_q}{dt} = \sum_k F^*_{jk}\beta^{(0)}_{q\ominus k}, \quad i\frac{d\beta^{(1)}_q}{dt} = \sum_k F_{jk}\alpha^{(0)}_{q\oplus k}, \tag{C1}$$

which then gives

$$\begin{aligned} \alpha^{(1)}_Q &= 1,\\ \alpha^{(1)}_q &= 0,\\ \beta^{(1)}_q &= -iF_{jk}t \ \text{ if } \ q = Q\ominus k. \end{aligned} \tag{C2}$$

These first-order solutions are then used again in the right-hand side of the coupled equations, to find the second-order solutions:

$$i\frac{d\alpha^{(2)}_q}{dt} = \sum_k F^*_{jk}\beta^{(1)}_{q\ominus k},$$
$$i\frac{d\beta^{(2)}_q}{dt} = \sum_k F_{jk}\alpha^{(1)}_{q\oplus k}, \tag{C3}$$

which then gives

$$\begin{aligned} \alpha^{(2)}_Q &= 1-\frac{1}{2}\left(\sum_k |F_{jk}|^2\right)t^2,\\ \alpha^{(2)}_q &= -\frac{1}{2}(F^*_{jk'}F_{jk})t^2 \ \text{ if } \ q = Q\ominus k\oplus k',\\ \beta^{(2)}_q &= -iF_{jk}t \quad \text{if} \quad q = Q\ominus k. \end{aligned} \tag{C4}$$

Using these second-order solutions, the third-order solutions can again be found by solving the coupled equations:

$$\begin{aligned}
\alpha_Q^{(3)} &= 1 - \frac{1}{2}\left(\sum_k |F_{jk}|^2\right)t^2, \\
\alpha_q^{(3)} &= -\frac{1}{2}(F_{jk'}^* F_{jk})t^2 \ \text{ if } \ q = Q \ominus k \oplus k', \\
\beta_q^{(3)} &= -i F_{jk} t + i\frac{1}{2}\frac{1}{3}\left(F_{jk}\sum_k |F_{jk}|^2\right)t^3 \\
&\quad + i\frac{1}{2}\frac{1}{3}\left(F_{jk}\sum_{k'} |F_{jk'}|^2\right)t^3 \ \text{ if } \ q = Q \ominus k, \\
\beta_q^{(3)} &= -i\frac{1}{2}\frac{1}{3}(F_{jk''}F_{jk'}^* F_{jk})t^3 \ \text{ if } \ q = Q \ominus k \oplus k' \ominus k''.
\end{aligned} \tag{C5}$$

This procedure can be continued until all coefficients of the Taylor series expansion for the initial probability amplitude $\alpha_Q(t)$ are found. As shown above, the solutions contain terms that are summations over the squares of the exchange coupling constants $\sum_k |F_{jk}|^2$, $\sum_{k'} |F_{jk'}|^2$, $\sum_{k''} |F_{jk''}|^2$, and so on. For the vast majority of the Hilbert space, these summations contain $\approx N/2$ terms. As the number of qubits N is increased, the expected value of these sums grows more quickly compared to the variations around the expected value. We, therefore, make the key assumption that in the $N \to \infty$ limit, these sums can be taken equal, $\sum_{j(q)} |F_{ij}|^2 \approx \sum_{j'} |F_{ij'}|^2 \approx \sum_{j''} |F_{ij''}|^2 \approx \cdots$ and replace these sums with their expected value $\sigma^2 = (NE'[F^2]/2)$. Under this assumption, the solution for the initial probability amplitude is of the form

$$\alpha_Q(t) = \sum_n (-1)^n \frac{l(n)}{(2n)!}(\sigma t)^{2n}, \tag{C6}$$

where the quantities $l(n)$ are combinatorial factors. By inspection, these factors can be found using the following recursive relationship. Start with an initial array of numbers A where the only nonzero element is the first element and it equals to 1; i.e., the initial array is $A^{(0)} = (1,0,0,0,0,0,\ldots)$. Then at each step, update the array using the recursive algorithm: $A^{(n)}(0) = A^{(n-1)}(0) + A^{(n-1)}(1)$, and $A^{(n)}(m) = A^{(n-1)}(m-1) + 2A^{(n-1)}(m) + A^{(n-1)}(m+1)$ for $m > 0$ (n is the number of iterations and m is the element number in the array). For example, after one iteration, the array is $A^{(1)} = (1,1,0,0,0,0,\ldots)$, after two iterations it is $A^{(2)} = (2,3,1,0,0,0,\ldots)$, and after three iterations, the array becomes $A^{(3)} = (5,9,5,1,0,0,\ldots)$, and so on. The combinatorial factors $l(n)$ are the first elements of the array at each iteration, $l(n) = A^{(n)}(1)$.

APPENDIX D: THE EIGENVALUE SPECTRUM OF THE TOTAL EXCHANGE HAMILTONIAN

Here we find the eigenvalue distribution of the exchange Hamiltonian $\hat{H}_{\text{eff}}$ in the limit of $N \to \infty$. We will use very similar techniques to those in Appendix B and use much of the same notation; for simplicity, when dealing with an object never referenced outside of the appendices, we use the same symbol for the analogous object from Appendix B, even though in some cases the analogous objects are not the same.

We again begin by calculating the moments of the distribution:

$$\sigma^{(m)} = 2^{-N}\text{Tr}[(\hat{H}_{\text{eff}})^m]. \tag{D1}$$

Following Appendix B, we introduce the basis $|q\rangle$ which correspond to definite arrangements q of all of the qubits in the computer. The set of all qubits is $\mathcal{N}$, and the set of all arrangements of any set of qubits $\mathcal{Q} \subseteq \mathcal{N}$ is denoted by $\mathcal{A}_\mathcal{Q}$; thus $q \in \mathcal{A}_\mathcal{N}$. We use the convention set in Appendix B for the form of arrangements which has explicit reference to the qubits involved. Each of the N qubits can be 0 or 1, which we call "lowered" and " raised" respectively, so $2^N = |\mathcal{A}_\mathcal{N}|$ is the number of elements in $\mathcal{A}_\mathcal{N}$. Expressing the trace in this basis results in

$$\sigma^{(m)} = 2^{-N}\sum_{q\in\mathcal{A}_\mathcal{N}} \langle q|(\hat{H}_{\text{eff}})^m|q\rangle. \tag{D2}$$

First we write each of the m Hamiltonians as a sum of pair Hamiltonians $\hat{H}_{\text{eff}} = \sum_{(kl)} \hat{H}^{kl}$, and then expand the product over the m Hamiltonians. Each term in the resulting expansion begins and ends with some state $|q\rangle$, and has m operators in between each of which act nontivially on two qubits, e.g., $\langle q|\hat{H}_{k_1l_1}\hat{H}_{k_2l_2}\ldots\hat{H}_{k_ml_m}|q\rangle$. For each sequence of m pairs of qubits $\{\{k_1l_1\}\{k_2l_2\}\ldots\{k_ml_m\}\}$, it is either the case that $\langle q|\hat{H}_{k_1l_1}\ldots\hat{H}_{k_ml_m}|q\rangle = 0$, in which case we call this sequence incompatible with the configuration $|q\rangle$, or else $\langle q|\hat{H}_{k_1l_1}\ldots\hat{H}_{k_ml_m}|q\rangle = F_{k_1l_1}F_{k_2l_2}\ldots F_{k_ml_m}$, in which case we call this sequence compatible with $|q\rangle$. Let $\mathcal{K}_\mathcal{Q}^m$ be the set of all sequences of m pairs of qubits chosen from the set $\mathcal{Q}$, and introduce a function $\omega(q \in \mathcal{A}_\mathcal{N}, \{\{k_1l_1\}\ldots\{k_ml_m\}\} \in \mathcal{K}_\mathcal{N}^m)$ which accepts states and sequences, and returns 1 if the sequence is compatible with the state and 0 if the sequence is incompatible with $|q\rangle$. Introducing the notation $\prod F(\{\{k_1l_1\}\ldots\{k_ml_m\}\} \in \mathcal{K}_\mathcal{Q}^m) = \prod_{\alpha=1}^m F_{k_\alpha l_\alpha}$, we then have

$$\begin{aligned}
\sigma^{(m)} &= 2^{-N}\sum_{q\in\mathcal{A}_\mathcal{N}}\sum_{(k_1l_1)}\sum_{(k_2l_2)}\cdots\sum_{(k_ml_m)} \langle q|\hat{H}_{k_1l_1}\hat{H}_{k_2l_2}\ldots\hat{H}_{k_ml_m}|q\rangle \\
&= 2^{-N}\sum_{q\in\mathcal{A}_\mathcal{N}}\sum_{(k_1l_1)}\sum_{(k_2l_2)}\cdots \\
&\quad \sum_{(k_ml_m)} \omega(q,\{\{k_1l_1\}\ldots\{k_ml_m\}\})\prod_{\alpha=1}^m F_{k_\alpha l_\alpha} \\
&= 2^{-N}\sum_{q\in\mathcal{N}}\sum_{K\in\mathcal{K}_\mathcal{N}^m} \omega(q,K)\prod F(K) \\
&= 2^{-N}\sum_{K\in\mathcal{K}_\mathcal{N}^m}\prod F(K)\sum_{q\in\mathcal{A}_\mathcal{N}} \omega(q,K).
\end{aligned} \tag{D3}$$

Let us divide the set $\mathcal{K}_\mathcal{Q}^m$ into subsets in which each element (sequence) has the same number of unique qubits appearing in it. We will denote the space of all sequences of m pairs of qubits chosen from the set $\mathcal{Q}$ with u unique qubits appearing in it by $\mathcal{K}_\mathcal{Q}^m(u)$. $\mathcal{K}_\mathcal{Q}^m = \mathcal{K}_\mathcal{Q}^m(1) \cup \mathcal{K}_\mathcal{Q}^m(2) \cup \cdots \cup \mathcal{K}_\mathcal{Q}^m(2m \wedge |\mathcal{Q}|)$ and $\mathcal{K}_\mathcal{Q}^m(u_1) \cap \mathcal{K}_\mathcal{Q}^m(u_2) = 0$ for $u_1 \neq u_2$, so we may express the sum over K as

$$\sigma^{(m)} = 2^{-N}\sum_{u=2}^{2m\wedge|\mathcal{N}|}\sum_{K\in\mathcal{K}_\mathcal{N}^m(u)}\prod F(K)\sum_{q\in\mathcal{A}_\mathcal{N}} \omega(q,K). \tag{D4}$$

We only require $\sigma^{(m)}$ out to arbitrarily high but finite order, so we take $2m \wedge |\mathcal{N}| = 2m \wedge N = 2m$.

We define $\mathcal{U}_K$ to be the unordered set of all qubits appearing in the sequence $K \in \mathcal{K}_Q^m$, so that $|\mathcal{U}_K| = u$ if $K \in \mathcal{K}_Q^m(u)$. For $\{\{k_1,l_1\},\ldots,\{k_m,l_m\}\} = K \in \mathcal{K}_Q^m$, the operator $\hat{H}_{k_1l_1}\ldots\hat{H}_{k_ml_m}$ acts nontrivially only on the qubits in $\mathcal{U}_K$, so for the same reasoning as in Appendix B, for a given $K \in \mathcal{K}_Q^m$ and $r \in \mathcal{A}_{\mathcal{U}_K}$, for any q,q' which are in $\mathcal{A}_\mathcal{N}$ and contain r (i.e., $q,q' \supseteq r$), $\omega(q,K) = \omega(q',K)$. Thus we may unambiguously define a new function $\tilde{\omega}(r \in \mathcal{A}_{\mathcal{U}_K}, K \in \mathcal{K}_Q^m(u))$, which accepts a sequence and arrangements of the qubits appearing in that sequence (as opposed to ω which accepts a sequence and arrangements of all N qubits), to be equal to $\omega(q,K)$ for any $q \supseteq r$, $q \in \mathcal{A}_\mathcal{N}$. For each sequence $K \in \mathcal{K}_Q^m(u)$, for any $r \in \mathcal{A}_{\mathcal{U}_K}$, there are 2^{N-u} unique $q \in \mathcal{A}_\mathcal{N}$ that contain r, because each of the $N-u$ qubits which are not in $\mathcal{U}_K$ can be up or down for such a q. Therefore, $\sum_{q\in\mathcal{A}_\mathcal{N}} \omega(q,K \in \mathcal{K}_\mathcal{N}^m(u)) = 2^{N-u}\sum_{r\in\mathcal{A}_{\mathcal{U}_K}} \tilde{\omega}(r,K)$, which allows us to write

$$\sigma^{(m)} = \sum_{u=2}^{2m} 2^{-u} \sum_{K\in\mathcal{K}_\mathcal{N}^m} \prod F(K) \sum_{r\in\mathcal{A}_{\mathcal{U}_K}} \tilde{\omega}(r,K). \tag{D5}$$

We wish to isolate the N dependence of the different pieces of this sum, so that we may keep only the important part as $N \to \infty$. To this end, note that we can construct any sequence $\{\{k_1,l_1\},\ldots,\{k_m,l_m\}\} = K \in \mathcal{K}_Q^m(u)$ out of (1) an ordered list of u subsets of the first m integers and (2) an ordered list of u unique qubits. The sequence is then constructed by assigning the first location in the sequence to the integer 1, the second to the integer 2, etc., and then placing the first qubit in the qubit list at all locations in the sequence associated with the integers contained in the first subset, the second qubit at all locations associated with integers in the second subset, and so forth until the uth qubit has been assigned. For example, the sequence $\{\{2,7\}\{5,9\}\{5,2\}\{7,9\}\{5,13\}\{5,13\}\}$ with $m = 6$ and $u = 5$ is constructed by the integer subsets $\{\{13\},\{5,6\},\{2,3,5,6\},\{1,4\},\{2,4\}\}$ and the qubit list $\{2,13,5,7,9\}$. A set of integer subsets paired with a qubit list generates a sequence as long as there are the same number of subsets as qubits, and each integer appears in exactly two subsets. We will call a set of integer subsets in which each integer appears in exactly two subsets a pattern, and denote the set of all patterns of m integers with u subsets by $\mathcal{S}_m(u)$, so that the set of all patterns of m integers is $\mathcal{S}_m = \mathcal{S}_m(2) \cup \mathcal{S}_m(3) \cup \cdots \cup \mathcal{S}_m(2m)$. We will call $\mathcal{L}_\mathcal{Q}^u$ the set of all ordered lists of u unique qubits chosen from the set of qubits $\mathcal{Q}$. We define a function K to take a pattern and a qubit list and return the constructed sequence; i.e., if $K \in \mathcal{K}_\mathcal{Q}^m(u)$ is the sequence constructed by $s \in \mathcal{S}_m(u)$ and $L \in \mathcal{L}_\mathcal{Q}^u$, then $K(s,L) = K$. The double use of the letter K should not lead to confusion, because after being given arguments, the function K becomes an element of $\mathcal{K}_\mathcal{N}^m$. Then, because every sequence can be constructed by some pattern and qubit list, we may express the moments as

$$\sigma^{(m)} = \sum_{u=2}^{2m} 2^{-u} \sum_{s\in\mathcal{S}_m(u)} \sum_{L\in\mathcal{L}_\mathcal{N}^u} \frac{1}{\Lambda(K(s,L))} \prod F(K(s,L)) \times \sum_{r\in\mathcal{A}_{\mathcal{U}_{S(s,L)}}} \tilde{\omega}(r,K(s,L)), \tag{D6}$$

where $\Lambda(K)$ is the number of combinations of patterns and qubit lists such which, when given as the argument of the function K, yields K. Each pattern and qubit list is associated with one sequence, but each sequence is associated with many pattern and qubit list combinations, so we must divide the degeneracy factor Λ to prevent overcounting. All sequences are paired uniquely with a set of subsets which make up a pattern; this is done by writing down subsets containing the integer locations of each qubit. The order is left arbitrary, and the sequence $K(s,L)$ will not be altered if we reorder the subsets in s and then reorder the qubits in L in the same way. Thus, $\Lambda(s) = u!$ for $s \in \mathcal{S}_m(u)$.

The system is invariant under the relabeling of qubits, so it must be that the quantity $\sum_{r\in\mathcal{A}_{\mathcal{U}_{K(s,L)}}} \tilde{\omega}(r,K(s,L)) \equiv \Omega(s)$ does not depend on choice of qubits, i.e., does not depend on L. This allows us to write

$$\sigma^{(m)} = \sum_{u=2}^{2m} \frac{1}{2^u u!} \sum_{s\in\mathcal{S}_m(u)} \Omega(s) \sum_{L\in\mathcal{L}_\mathcal{N}^u} \prod F(K(s,L)). \tag{D7}$$

In evaluating Eq. (D7), we note that there is no N dependence in $|\mathcal{S}_m(u)|$ or $\Omega(s)$. Thus for fixed m, the above sum is a fixed number of terms (one for each pattern $s \in \mathcal{S}_m$), with a fixed coefficient (equal to $\Omega(s)/2^u u!$) in front of an N-dependent sum $\sum_{L\in\mathcal{L}_\mathcal{N}^u} \prod F(K(s,L)) \equiv G_s(N)$:

$$\sigma^{(m)} = \sum_{u=2}^{2m} \frac{1}{2^u u!} \sum_{s\in\mathcal{S}_m(u)} \Omega(s) G_s(N). \tag{D8}$$

Having isolated the N dependence, we wish to identify the parts with the largest scaling, since we need only keep these as $N \to \infty$ in order to have a quantity which fractionally converges to $\sigma^{(m)}$ for large N. First, we subdivide each set $\mathcal{S}_m(u)$ into sets $\mathcal{S}_m(u,v)$ where v is the number of pairs of subsets in s whose intersects contain an odd number of integers. Intuitively, this is the number of qubits whose choice in L will affect the overall sign of $\prod F(K(s,L))$ because that qubit appears as the index of an F which appears an odd number of times in $\prod F$ in total. Each element of $\mathcal{S}_m(u)$ belongs in one such $\mathcal{S}_m(u,v)$, so we can write

$$\sigma^{(m)} = \sum_{u=2}^{2m} \frac{1}{2^u u!} \sum_{v=0}^{u} \sum_{s\in\mathcal{S}_m(u,v)} \Omega(s) G_s(N). \tag{D9}$$

We now examine the scaling with large N of the sums $\sum_{L\in\mathcal{L}_\mathcal{N}^u} \prod F(S(s,L)) \equiv G_s(N)$ for patterns with nonzero coefficients, i.e., $\Omega(s) \neq 0$, since only these have relevant N scaling. We use the notation $A \to B$ to mean that A fractionally converges to B, i.e., $A/B = 1$ in the limit that N goes to infinity. In addition, $<_N$ means "has lower N scaling than," so that if $A/B \to 0$, then it must be that $A <_N B$. In order for $\Omega(s) \neq 0$, each subset in s must contain an even number of integers, so that every qubit gets flipped an even number of times and therefore is ultimately unchanged, allowing $\langle q|\hat{H}_{k_1l_1}\ldots\hat{H}_{k_ml_m}|q\rangle \neq 0$. Thus $\Omega(s \in \mathcal{S}_m(u > m)) = 0$, and so we may truncate the sum over u at m. We note that $\mathcal{L}_\mathcal{N}^u$ is the set of all ways to make an ordered list of u unique qubits chosen from the set of all qubits, so $|\mathcal{L}_\mathcal{N}^u| = \binom{N}{u}u! \to N^u$ is the number of ways to pick u qubits times the number of ways to order them. Thus, by the definition of the expectation value of

a pattern $E_s[\prod F]$ as defined in Appendix F, for $s \in \mathcal{S}_m(u,v)$ we have

$$G_s(N) = \sum_{L\in\mathcal{L}^u_N} \prod F(S(s,L)) = \frac{N!}{(N-u)!} E_s\Big[\prod F\Big] \to N^u E_s\Big[\prod F\Big]. \quad \text{(D10)}$$

When $v \neq 0$, in the large sample limit where the sign of each F_{jk} factor is random, $G_s(N) \to 0$. However, for purposes of comparing the relative size of terms, we are interested in the typical size of $G_s(N)$, denoted by $|G_s(N)|$, which by the central limit theorem has the typical size

$$|G_s(N)| \to N^{u-v}\sqrt{N^v} E_s\Big[\Big|\prod F\Big|\Big] = N^{u-v/2} E_s\Big[\Big|\prod F\Big|\Big]. \quad \text{(D11)}$$

For $v = 0$, $|G_s(N)| = G_s(N)$ since each term in the sum is positive.

We proceed to identify the class of patterns for which $|G_s(N)|$ has the largest N scaling among all s with $\Omega(s) \neq 0$ by taking certain kinds of patterns s and identifying patterns s' for which $|G_s(N)| <_N |G_{s'}(N)|$; then, as long as $\Omega(s') \neq 0$, the $|G_s(N)|$ term can be ignored in the large-N limit since they will become negligible compared to the $|G_{s'}(N)|$ term. For each of the steps below, we choose s' related to s such that $\Omega(s) \neq 0 \Rightarrow \Omega(s') \neq 0$.

We begin with patterns in which there exists a pair of subsets whose intersect contains greater than two elements; this means that for any $L \in \mathcal{L}^u_N$, in $\prod F(S(s,L))$ is some F^a_{jk} for $a > 2$, where j and k are decided by L. Let s' be the pattern created by starting with s, finding two subsets with an intersect larger than two, choosing any two elements of that intersection and removing them from both subsets, then creating two new subsets, each of which contains both elements. This effectively takes F^a_{jk} to $F^{a-2}_{jk}F^2_{j'k'}$, where j' and k' do not appear anywhere else in the sequence. As shown in Appendix F, when s and s' have this relationship, $E_s[|\prod F|] < N E_{s'}[|\prod F|]$, meaning that

$$|G_s(N)| \to N^{u-v/2} E_s\Big[\Big|\prod F\Big|\Big] < N^{u+1-v/2} E_{s'}\Big[\Big|\prod F\Big|\Big] = N^{u'-1-v'/2} E_{s'}\Big[\Big|\prod F\Big|\Big] \to N^{-1}|G_{s'}(N)|, \quad \text{(D12)}$$

where $s \in \mathcal{S}_m(u,v)$ so $s' \in \mathcal{S}_m(u',v') = \mathcal{S}_m(u+2,v)$. Thus terms associated with s can be ignored in the large-N limit, and we now focus only patterns for which the overlap between any two subsets contains at most two integers; i.e., for each unique F_{jk} in $\prod F(s,L)$, it is either raised to the first or second power.

Next we show that any pattern with a subset containing four or more elements that has two elements in an intersect with another subset can be ignored. The products associated with these patterns contain terms like $F_{k_1k_2}F^2_{k_2k_3}$, and we show that these scale less with N then the same pattern but with this product changed to $F_{k_1k_2}F^2_{k_3k_4}$. Accordingly, let us call the original pattern s, and s' the pattern s except with the two elements in the intersect between the subset with four or more elements, another subset removed from both, and both added to two new subsets which contains only those two elements. Note that for $s \in \mathcal{S}_m(u,v)$ and $s' \in \mathcal{S}_m(u',v')$, $v' = v$ while $u' = u+2$ or $u+1$, the latter case being if the subset in s whose intersect with a subset with four or more elements contains two elements has only two elements in it in total. According to Appendix F, $E_s[|\prod F|] <_N N E_{s'}[|\prod F|]$, which yields for $s \in \mathcal{S}_m(u,v)$ and $s' \in \mathcal{S}_m(u',v')$,

$$|G_s(N)| \to N^{u-v/2} E_s\Big[\Big|\prod F\Big|\Big] <_N N^{1+u-v/2} E_{s'}\Big[\Big|\prod F\Big|\Big] \leqslant N^{u'-v'/2} E_{s'}\Big[\Big|\prod F\Big|\Big] \to |G_{s'}(N)|. \quad \text{(D13)}$$

Thus terms associated with patterns like s can be ignored.

The only patterns that have not been shown to be ignorable for large N have at most two elements in the intersect of any two of its subsets, and if the intersect between two subsets does contain two elements than both subsets contain only two elements. This corresponds to patterns with $\prod F(K(s,L))$ of the form $F_{k_1k_2}F_{k_2k_3}F_{k_3k_1}F^2_{k_4k_5}F^2_{k_6k_7}$, where there are a number of F^2 with no overlapping indices, and then a number of F^1 with potentially complicated overlapping indices with each other but not with any of the F^2. For one of these patterns $s \in \mathcal{S}_m(u,v)$, let us call a the number of pairs of subsets whose intersect contains two elements (i.e., the number of F^2 in $\prod F(K(s,L))$, so that $2a = u - v$), and let $b = m - 2a$ be the number of F^1 which appear in $\prod F(K(s,L))$. All qubits appearing as an argument of an F^1 can affect the overall sign, while the ones appearing in an F^2 cannot, so $v \leqslant b$.

We first treat the case that m is even; note in this case that b is even. Let $s' \in \mathcal{S}_m(m,0)$ be a pattern in which all subsets contain two elements, and the intersect between any two subsets contains 2 or 0 elements. This corresponds to patterns with $\prod F(K(s',L))$ of the form $F^2_{k_1k_2}F^2_{k_3k_4}\ldots F^2_{k_{m-1}k_m}$. $G_{s'}(N)$ is the same for all s' which obey this property because they are all the same under the renaming and reordering of qubits and subsets, and we call this $G_{(2,m)}(N)$. If $b = 0$, then $G_s(N) = G_{(2,m)}(N)$. In Appendix F, it is shown for $b \neq 0$ that $E_s[|\prod F|] < N^{b/2-1/2}E_{s'}[|\prod F|] = N^{b/2-1/2}E_{s'}[\prod F]$, which means that for $s \in \mathcal{S}_m(u,v)$ and $s' \in \mathcal{S}_m(m,0)$,

$$|G_s(N)| \to N^{u-v/2} E_s\Big[\Big|\prod F\Big|\Big] < N^{u-v/2+b/2-1/2} E_{s'}\Big[\prod F\Big] = N^{u-v/2+b/2-1/2-m} G_{s'}(N) = N^{u-v/2+b/2-1/2-m} G_{(2,m)}(N). \quad \text{(D14)}$$

Using the relations $2a + b = m$ and $2a + v = u$, we have that $u - v/2 + b/2 - m = \frac{1}{2}(v - b)$, and since $v \leqslant b$, $u - v/2 + b/2 - m \leqslant 0$, allowing us to conclude

$$|G_s(N)| < N^{-1/2} G_{(2,m)}(N), \quad \text{(D15)}$$

meaning that, for m even, only patterns with all subsets containing 2 elements and all intersects containing 2 or 0 elements matter as $N \to \infty$, and all of these matter because the terms associated with each of these patterns have the same N scaling. These are exactly the patterns in $\mathcal{S}_m(m,0)$, so

$$\sigma^{(m)} \to \frac{1}{2^m m!} \sum_{s\in\mathcal{S}_m(m,0)} \Omega(s) G_s(N) = \frac{1}{2^m m!} G_{(2,m)}(N) \sum_{s\in\mathcal{S}_m(m,0)} \Omega(s), \quad m \text{ even}. \quad \text{(D16)}$$

Now we treat the case that m is odd; note in this case that b is odd. Let $s' \in \mathcal{S}_m(u,3)$ be a pattern in which all but three subsets contain two elements, and the intersect between any two of these subsets contains 2 or 0 elements, and the other three subsets each have 2 elements and the intersect between any two of them contains 1 element. For all such s', the N scaling of $|G_{s'}(N)|$ is the same, and we call this $|G_{(3,m)}(N)|$. In Appendix F, it is shown that, for $b > 3$, $E_s[|\prod F|] <_N N^{b/2-3/2} E_{s'}[|\prod F|]$, and therefore

$$\begin{aligned} |G_s(N)| &\to N^{u-v/2} E_s\left[\left|\prod F\right|\right] <_N N^{u-v/2+b/2-3/2} E_{s'}\left[\left|\prod F\right|\right] \\ &\to N^{u-v/2+b/2-3/2-(m-3/2)} |G_{s'}(N)| = N^{u-v/2-m+b/2} |G_{(3,m)}(N)|. \end{aligned} \tag{D17}$$

Using the same relation as in the m even case, that $u - v/2 + b/2 - m = \frac{1}{2}(v-b) \leqslant 0$, we conclude

$$|G_s(N)| <_N |G_{(3,m)}(N)|, \tag{D18}$$

and thus for m odd, only patterns like s' described above matter as $N \to \infty$. These are exactly all of the patterns in $\mathcal{S}_m(u,3)$, so for m odd, the typical size of the moments scales as

$$|\sigma^{(m)}| \to \frac{1}{2^m m!} \sum_{s \in \mathcal{S}_m(m,0)} \Omega(s) |G_s(N)| = \frac{1}{2^m m!} |G_{(3,m)}(N)| \sum_{s \in \mathcal{S}_m(m,3)} \Omega(s), \quad m \text{ odd}. \tag{D19}$$

Now we must evaluate $\Omega(s)$ for $s \in \mathcal{S}_m(m,3)$ when m is odd, and $s \in \mathcal{S}_m(m,0)$ when m is even. Recall that $\Omega(s) = \sum_{r \in \mathcal{A}_{U_K(s,L)}} \tilde{\omega}(r, K(s,L))$ for any $L \in \mathcal{L}^m_{\mathcal{N}}$ is the number of arrangements of the set L of m qubits such that the Hamiltonian operator term associated with the sequence $K(s,L)$ (for example, if $K(s,L) = \{\{k_1,l_1\}, \ldots, \{k_m l_m\}\}$ then the associated operator term is $\hat{H}_{k_1 l_1} \ldots \hat{H}_{k_m l_m}$), when sandwiched in between $\langle q||q\rangle$ for any $q \supset r$, is not zero. In order for $\langle q|\hat{H}_{k_1 l_1} \ldots \hat{H}_{k_m l_m}|q\rangle \neq 0$, k_1 can have any status in q but l_1 must be opposite k_1. Similarly, for each pair of qubits which appear as indices on the same Hamiltonian, they must be opposite one another, and so there are two choices. For $s \in \mathcal{S}_m(m,0)$, if k_1 and l_1 appear as indices on a Hamiltonian, then they also appear on the indices on another Hamiltonian, and the condition is therefore automatically satisfied for the second. There are $m/2$ pairs of qubits, so $\Omega(s) = 2^{m/2}$. For $s \in \mathcal{S}_m(m,3)$, the same reasoning applies to each paired Hamiltonian, of which there are $(m-3)/2$. For the triplet of the form $H_{k_1 k_2} H_{k_2 k_3} H_{k_3 k_1}$, once the status of k_1 is set, the status of k_2 and k_3 is fixed, so all three of those qubits only contribute a factor of 2 to $\Omega(s)$. Thus $\Omega(s) = 2^{(m-3)/2} \times 2 = 2^{m/2-1/2}$, and

$$\begin{aligned} \sigma^{(m)} &\to \frac{1}{2^m m!} G_{(2,m)}(N) \sum_{s \in \mathcal{S}_m(m,0)} 2^{m/2} = \frac{1}{2^{m/2} m!} G_{(2,m)}(N) |\mathcal{S}_m(m,0)|, \quad m \text{ even}, \\ |\sigma^{(m)}| &\to \frac{1}{2^m m!} |G_{(3,m)}(N)| \sum_{s \in \mathcal{S}_m(m,3)} 2^{m/2-1/2} = \frac{1}{2^{m/2+1} m!} |G_{(3,m)}(N)| |\mathcal{S}_m(m,3)|, \quad m \text{ odd}. \end{aligned} \tag{D20}$$

For m even, elements of $\mathcal{S}_m(m,0)$ have $m/2$ unique subsets which each contain two integers, and there are two copies of each subset. Thus $|\mathcal{S}_m(m,0)|$ is the number of ways to pair up m objects times the number of ways to order the m objects. There are $\binom{m}{2}\binom{m-2}{2} \ldots \binom{4}{2}\binom{2}{2} = 2^{-m/2} m!$ ways to pair up the Hamiltonian terms, and $m!$ ways to order them, so $|S_m(m,0)| = 2^{-m/2}(m!)^2$. For m odd, elements of $\mathcal{S}_m(m,3)$ have $(m-3)/2$ unique subsets which each contain two integers, and there are two copies of each of these: The other three subsets each contain two elements, and the intersect with each other contains one element. Thus $|\mathcal{S}_m(m,3)|$ is the number of ways to choose three objects from m of them times the number of ways to pair up $m-3$ objects times the number of ways to order all m of them, which is $\binom{m}{3} \times 2^{-(m-3)/2}(m-3)! \times m! = \frac{1}{3} 2^{-m/2+1/2}(m!)^2$. Therefore,

$$\begin{aligned} \sigma^{(m)} &\to \frac{1}{2^{m/2} m!} G_{(2,m)}(N) 2^{-m/2} (m!)^2 = \frac{m!}{2^m} G_{(2,m)}(N), \quad m \text{ even}, \\ |\sigma^{(m)}| &\to \frac{1}{2^{m/2+1} m!} |G_{(3,m)}(N)| \frac{1}{3} 2^{-m/2+1/2} (m!)^2 = \frac{1}{3\sqrt{2}} \frac{m!}{2^m} |G_{(3,m)}(N)|, \quad m \text{ odd}. \end{aligned} \tag{D21}$$

We next discuss how the odd moments can be ignored in the $N \to \infty$ limit by evaluating the moment generating function, which is the Fourier transform of the probability density function of the eigenvalue distribution:

$$\begin{aligned} F_{\text{moment}}(\zeta) &= \sum_{m=0}^{\infty} \frac{(i\zeta)^m}{m!} \sigma^{(m)} = \sum_{m=0}^{\infty} \left(\frac{(is)^{2m}}{(2m)!} \sigma^{(2m)} + \frac{(i\zeta)^{2m+1}}{(2m+1)!} \sigma^{(2m+1)} \right) = \sum_{m=0}^{\infty} \frac{(i\zeta)^{2m}}{(2m)!} \left(\sigma^{(2m)} + \frac{i\zeta}{2m+1} \sigma^{(2m+1)} \right) \\ &= \sum_{m=0}^{\infty} (i\zeta/2)^{2m} \left(G_{(2,2m)}(N) + \frac{i\zeta}{6\sqrt{2}} G_{(3,2m+1)}(N) \right). \end{aligned} \tag{D22}$$

As in Appendix F, we define $E_{(2,m)}[\prod F]$ by $G_{(2,m)} \to N^m E_{(2,m)}[\prod F]$ and similarly $|G_{(3,m)}| \to N^m E_{(3,m)} E[|\prod F|]$. Using the result that $E_{(2,m)}[\prod F] \to E[F^2]^{m/2}$, $G_{(2,m)}(N) \to N^m E[F^2]^{m/2}$, and introducing the rescaled variable $\tilde{\zeta} = N E[F^2]^{1/2} \zeta$, we

obtain

$$F_{\text{moment}}(\tilde{\zeta}) = \sum_{m=0}^{\infty} (i\tilde{\zeta}/2)^{2m} \left(1 + \frac{i\tilde{\zeta}}{6\sqrt{2}} \frac{G_{(3,2m+1)}}{N^{2m+1} E[F^2]^{m+1}}\right). \tag{D23}$$

Typically, the size of $G_{(3,m)}(N)$ is $|G_{(3,m)}(N)| \to N^{m-3/2} E_{(3,m)}[|\prod F|]$. As shown in Appendix F, the N scaling of $E_{(3,m)}[|\prod F|]$ is at most $E_{(2,m-3)}[\prod F] \times E[|F|] \to E[|F|]E[F^2]^{(m-3)/2}$, and so $|G_{(3,2m+1)}(N)|/(N^{2m+1}E[F^2]^{m+1})$ has, as a maximum N scaling, $N^{2m+1-3/2} \times E[|F|]E[F^2]^{(2m+1-3)/2}/(N^{2m+1}E[F^2]^{m+1}) = E[|F|]/(N^{3/2}E[F^2]^2)$. As shown in Appendix E, in 2D geometry, $E[F^2] \sim \ln(N)/N$ and $E[|F|] \sim N^{-1/2}$, so this maximum N scaling is $\ln(N)^{-2}$, which vanishes when compared to the other term which ~ 1. Similarly, in 3D geometry, $E[F^2] \sim N^{-2/3}$ and $E[|F|] \sim N^{-1/3}$, and so the maximum N scaling is $N^{-1/2}$ which also vanishes when compared to the other term. Thus the odd terms can be ignored in the large-N limit, and the moment generating function converges to

$$F_{\text{moment}}(\tilde{\zeta}) \to \sum_{m=0}^{\infty} (i\tilde{\zeta}/2)^{2m} = \sum_{m=0}^{\infty} (i\zeta N E[F^2]^{1/2}/2)^{2m}. \tag{D24}$$

APPENDIX E: THE DISTRIBUTIONS AND EXPECTATION VALUES OF VARIOUS POWERS OF THE EXCHANGE COUPLING CONSTANTS

In this Appendix, we discuss the probability density functions and the expectation values of various powers of the exchange coupling constants F_{jk} for both the 2D and 3D geometries. We are particularly interested in the N dependence of the expected values of these quantities in the $N \to \infty$ limit since these expected values are used throughout the paper. The full expression for the exchange coupling constants are given in Eq. (5). Since we are interested in the $N \to \infty$ limit, we will only consider the leading order of these constants, $F_{jk} \propto \sin \kappa_a r_{jk}/(\kappa_a r_{jk})$. For large distances, the $\sin \kappa_a r_{jk}$ term essentially produces a random sign, whose square contributes a factor of $1/2$ to the expected value. We therefore focus on the remaining $1/(\kappa_a r_{jk})$ term in this section. We define a random variable $U \equiv 1/(\kappa_a^2 r_{jk}^2)$ (which is proportional to the square of the exchange coupling constant $U \sim F_{jk}^2$) and first discuss the probability density function and the expected value of this random variable. We will then discuss the distributions and the expected values of various powers of U.

1. Two-dimensional geometry

Consider a two-dimensional array of qubits in a square geometry, in x-y dimensions. Note that $r_{jk}^2 = x_{jk}^2 + y_{jk}^2 = (x_j - x_k)^2 + (y_j - y_k)^2$ where (x_j, y_j) and (x_k, y_k) are the coordinates of the jth and kth qubits respectively. We view each of these coordinates x_j, x_k, y_j, and y_k to be uniformly distributed random variables within the interval $[0 \;\; N^{1/2}d]$. Taking these initial uniformly distributed random variables, the probability density function of the random variable $U \equiv 1/(\kappa_a^2 r_{ij}^2)$ can be found using the methods outlined in Ref. [65]. Defining $f_U(u)du \equiv P\{u \leqslant U \leqslant u + du\}$, this probability density function is

$$\begin{aligned} f_U(u) &= 0 \quad \text{if } u < 0 \\ &= 0 \quad \text{if } 0 \leqslant u \leqslant \frac{1}{2L^2} \\ &= \frac{1}{u^2}\left[\frac{2}{L^2}\arcsin(2L^2u - 1) - \frac{2}{L^2} - \frac{1}{uL^4} + \frac{4}{L^3}\sqrt{\frac{1}{u} - L^2}\right] \quad \text{if } \frac{1}{2L^2} \leqslant u \leqslant \frac{1}{L^2} \\ &= \frac{1}{u^2}\left[\frac{\pi}{L^2} + \frac{1}{uL^4} - \frac{4}{\sqrt{u}L^3}\right] \quad \text{if } \frac{1}{L^2} \leqslant u \leqslant \frac{1}{\kappa_a^2 d^2}. \end{aligned} \tag{E1}$$

Here, the quantity $L \equiv N^{1/2}\kappa_a d$ is the phase accumulation over the full length of the square. Using the density function of Eq. (E1), the expectation value of U can be found, which gives in the $N \to \infty$ limit

$$E[U] = \int f_U(u) u du = \frac{\pi}{\kappa_a^2 d^2} \frac{\ln N}{N}. \tag{E2}$$

Using the probability density function of the random variable U, we can find the distributions of various powers of U (such as $\sqrt{U}$, $U^{3/2}$, and so on) again using the methods outlined in Ref. [65]. These distributions are then used to find the corresponding expected values various powers of the exchange coupling constants. These results are

$$\begin{aligned} E[|F|] &= \frac{\Gamma}{\kappa_a d} \frac{2\pi - \frac{10}{3}}{N^{1/2}}, \\ E[F^2] &= \pi \frac{\Gamma^2}{\kappa_a^2 d^2} \frac{\ln N}{N}, \\ E[F^n] &\sim \frac{\Gamma^n}{\kappa_a^n d^n} \frac{1}{N} \quad \text{for } n > 2. \end{aligned} \tag{E3}$$

2. Three-dimensional geometry

Here, we consider a three-dimensional array of cubits in a cube geometry, in x-y-z dimensions and we have $r_{jk}^2 = x_{jk}^2 + y_{jk}^2 + z_{jk}^2 = (x_j - x_k)^2 + (y_j - y_k)^2 + (z_j - z_k)^2$. Following the above discussion, taking all the coordinates to be uniformly distributed, the probability density function of $U \equiv 1/(\kappa_a^2 r_{jk}^2)$ is

$$
\begin{aligned}
f_U(u) &= 0 \quad \text{if } u < 0 \\
&= 0 \quad \text{if } 0 \leqslant u \leqslant \frac{1}{3L^2} \\
&= \frac{1}{u^2}\int_{1/u-L^2}^{2L^2}\left[\frac{2}{L^2}\arcsin\left(\frac{2L^2-t}{t}\right) - \frac{2}{L^2} - \frac{t}{L^4} + \frac{4\sqrt{t-L^2}}{L^3}\right]\left[\frac{1}{\sqrt{\frac{1}{e}-tL}} - \frac{1}{L^2}\right]dt \quad \text{if } \frac{1}{3L^2} \leqslant u \leqslant \frac{1}{2L^2} \\
&= \frac{1}{u^2}\int_{1/u-L^2}^{L^2}\left[\frac{\pi}{L^2} + \frac{t}{L^4} - \frac{4\sqrt{t}}{L^3}\right]\left[\frac{1}{\sqrt{\frac{1}{u}-tL}} - \frac{1}{L^2}\right]dt \\
&\quad + \frac{1}{u^2}\int_{L^2}^{1/u}\left[\frac{2}{L^2}\arcsin\left(\frac{2L^2-t}{t}\right) - \frac{2}{L^2} - \frac{t}{L^4} + \frac{4\sqrt{t-L^2}}{L^3}\right]\left[\frac{1}{\sqrt{\frac{1}{u}-tL}} - \frac{1}{L^2}\right]dt \quad \text{if } \frac{1}{2L^2} \leqslant u \leqslant \frac{1}{L^2} \\
&= \frac{1}{u^2}\left[\frac{2\pi}{\sqrt{u}L^3} - \frac{3\pi}{eL^4} + \frac{4}{u\sqrt{e}L^5} - \frac{1}{2u^2L^6}\right] \quad \text{if } \frac{1}{L^2} \leqslant u \leqslant \frac{1}{\kappa_a^2 d^2}.
\end{aligned}
\tag{E4}
$$

Here, the probability density function in some of the regions cannot be evaluated analytically and as a result they are left in the integral form (the quantity t is the integration variable). The quantity $L \equiv N^{1/3}\kappa_a d$ is again the phase accumulation over one length of the cube. We numerically find that for the calculation of the expectation value, the majority of the contribution comes from the $\frac{1}{L^2} \leqslant u \leqslant \frac{1}{\kappa_a^2 d^2}$ region which can be evaluated analytically:

$$
E[U] = \int f_U(u) u du = \left(\pi + \frac{29}{12}\right)\frac{1}{\kappa_a^2 d^2}\frac{1}{N^{2/3}}. \tag{E5}
$$

The exact numerical result that includes all the regions of the probability density function [given in Eq. (E4)] differs from the analytical result of Eq. (E5) only by 1.2%. Following the 2D discussion, with the probability density function $f_U(u)$ known, the distribution of the various powers of U can be evaluated and the corresponding expectation values for the coupling constants are (again with an accuracy at the level of few percent)

$$
\begin{aligned}
E[|F|] &= \frac{\Gamma}{\kappa_a d}\frac{2\pi - \frac{9}{5}}{N^{1/3}}, \\
E[F^2] &= \left(\pi + \frac{29}{12}\right)\frac{\Gamma^2}{\kappa_a^2 d^2}\frac{1}{N^{2/3}}, \\
E[F^3] &= \frac{4\pi}{3}\frac{\Gamma^3}{\kappa_a^3 d^3}\frac{\ln N}{N}, \\
E[F^n] &\sim \frac{\Gamma^n}{\kappa_a^n d^n}\frac{1}{N} \quad \text{for } n > 3.
\end{aligned}
\tag{E6}
$$

In Fig. 8, we plot the probability density function $f_U(u)$ for both the 2D (dashed red line) and 3D (black solid line) geometries. The functions are plotted for the case when the length of each side is $L = 1$. For an arbitrary L, the horizontal axis of the plot is scaled by $1/L^2$ whereas the vertical axis is scaled by L^2.

In the above discussion, we have taken selected qubits j and k to be randomly among all the qubits and have calculated the distribution and the expected value of the exchange coupling constants F_{jk}. For the single-qubit error Hamiltonian and subsequent discussion, one of the qubits, qubit j, is fixed, and the summations are over the remaining qubits in the computer. For this case, the precise values of the distributions and the expected values will depend on the choice of the qubit j, for example, whether it is chosen to be at the edge of the array or at the center. However, using the above formalism, as expected, one can show that these considerations do not change the N scalings of the expected values, i.e., $E'[F^n] \sim E[F^n]$ for all n in both 2D and 3D geometries.

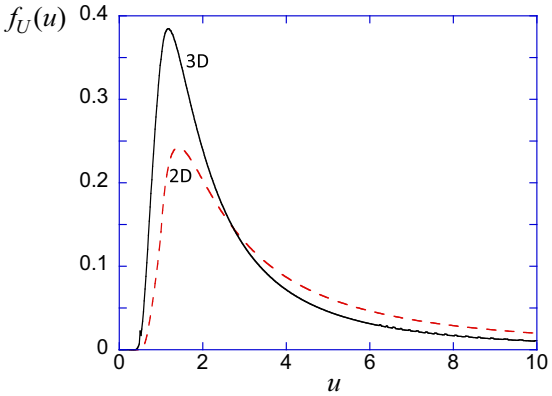

FIG. 8. The probability density functions of the random variable $U \equiv 1/(k_a^2 r_{ij}^2)$ for an array of atoms in two (dashed red line) and three (solid black line) dimensions. The functions are plotted for the case when the length of each side is $L = 1$. For an arbitrary L, the horizontal axis of the plot is scaled by $1/L^2$ whereas the vertical axis is scaled by L^2.

APPENDIX F: VARIOUS DEFINITIONS AND RESULTS ON THE EXPECTED VALUES OF THE COUPLING CONSTANTS

In this Appendix, we define the expectation values $E_s[\prod F]$ and $E'_s[\prod F]$ for some pattern of u subsets of m integers $\mathcal{S}_m(u)$ (see Appendixes B and D for this and other definitions used in this Appendix). The expectation value is over all ways to choose qubits for the pattern, i.e., over all qubit lists which can combine with that pattern to create a sequence. In the single-qubit Hamiltonian case, we only choose qubits from $\mathcal{N}'$, which is the set of all qubits besides j, whereas in the full Hamiltonian case we choose qubits from $\mathcal{N}$, which is the set of all qubits. Thus we define two expectation values, one for each case: For $s \in \mathcal{S}_m(u)$,

$$E_s\Big[\prod F\Big] = \sum_{L\in\mathcal{L}^u_{\mathcal{N}}} \prod F(S(s,L))/\big|\mathcal{L}^u_{\mathcal{N}}\big|, \quad E'_s\Big[\prod F\Big] = \sum_{L\in\mathcal{L}^u_{\mathcal{N}'}} \prod F(S(s,L))/\big|\mathcal{L}^u_{\mathcal{N}'}\big|. \tag{F1}$$

We can divide the sum over all elements of $\mathcal{L}^u_{\mathcal{Q}}$ into a sum over all ways to choose qubits from $\mathcal{Q}$ and a sum over all ways to order those qubits. This implies that $|\mathcal{L}^u_{\mathcal{Q}}| = \binom{|\mathcal{Q}|}{u} u! = |\mathcal{Q}|!/(|\mathcal{Q}|-u)!$, which scales as N^u when $\mathcal{Q} = \mathcal{N}$ or $\mathcal{N}'$. Taking this limit, and denoting the sum over all choices of u qubits from the set $\mathcal{Q}$ by $\sum^{(\mathcal{Q})}_{(k_1\ldots k_u)}$, the sum over all permutations of these qubits by $\sum_{\pi_u}$, and the element of $\mathcal{L}^u_{\mathcal{Q}}$ created by putting the qubits $k_1 \ldots k_u$ in the order π_u by $L(\{k_1 \ldots k_u\},\pi_u)$,

$$\begin{aligned} E_s\Big[\prod F\Big] &\to N^{-u} \sum_{(k_1\ldots k_u)}^{(\mathcal{N})} \sum_{\pi_u} \prod F(S(s,L(\{k_1 \ldots k_u\},\pi_u))), \\ E'_s\Big[\prod F\Big] &\to N^{-u} \sum_{(k_1\ldots k_u)}^{(\mathcal{N}')} \sum_{\pi_u} \prod F(S(s,L(\{k_1 \ldots k_u\},\pi_u))). \end{aligned} \tag{F2}$$

We also define

$$\begin{aligned} E'[F^2] &= \frac{1}{N-1}\sum_{k\neq j} F^2_{jk} \to N^{-1}\sum_{k\neq j} F^2_{jk}, \\ E[F^2] &= \frac{1}{\binom{N}{2}}\sum_{(kl)} F^2_{kl} \to N^{-2}\sum_{k}\sum_{l\neq k} F^2_{kl}, \\ E[|F|] &= \frac{1}{\binom{N}{2}}\sum_{(kl)} |F_{kl}| \to N^{-2}\sum_{k}\sum_{l\neq k} |F_{kl}|. \end{aligned} \tag{F3}$$

The N scalings of the expected values of Eq. (F3) are discussed in Appendix E. Next, we prove inequalities between expectation values of patterns related in specific ways. We will utilize the N scaling of the maximum and minimum values of $F(x) = f\frac{\sin(kx)}{kx}$ in the large sample size limit where the the sine can be averaged out, leaving $|F(x)| = \tilde{f}/kx$. In this case, $F_{\max} = \tilde{f}/kd$, and $F_{\min} = \tilde{f}/kR \sim N^{-1/D}$, where R is the largest separation between any two qubits, and the computer dimension is D, so that R scales as $N^{1/D}$. This means that, for any x and y, $|F(x)| \leqslant N^{1/D}|F(y)|$, where the equality is only if $x = d$ and $y = R$. This also means that, for any k_1,l_1,k_2,l_2, $|F_{k_1l_1}| \leqslant N^{1/D}|F_{k_2l_2}|$.

As mentioned previously, we will make use of the notation $A <_N B$ which means that the N scaling of A is less than the N scaling of B, i.e., $A/B \to 0$ as $N \to \infty$. We also define $\sim$ to mean " scales with N as": For example, $A \sim N^a$ means that $A \to cN^a$ for some constant c.

For the single-qubit case, if we call the number of integers in subset z p_z, then we may associate with each pattern a list of integers $\{p_1,\ldots,p_u\}$ for which $\sum_{z=1}^u p_z = m$. All patterns which are compatible with any states (i.e., $\Omega(s) \neq 0$) have an even number of integers in each of its u subsets; i.e., p_z is even for all z. We seek to show that for any s with $\{p_1,\ldots,p_i,\ldots p_u\}$ with some $p_i > 2$, $E'_s[\prod F] <_N NE'_{s'}[\prod F]$ where s' has $\{p_1,\ldots,p_i-2,\ldots,p_u,2\}$. This is done by using the definitions of the the expectation values, and that $F^2_{jk_1} < N^{2/D}F^2_{jk_2}$ for any k_1 and k_2, which is a consequence of the inequality established above. Defininings $\sum'_{k_i}$ to be $\sum_{k_i\neq k_1,\ldots,k_{i-1}}$, we have

$$\begin{aligned} E'_s\Big[\prod F\Big] &\to N^{-u}\sum_{(k_1\ldots k_u)}^{(\mathcal{N}')}\sum_{\pi_u}\prod F(S(s,L(\{k_1\ldots k_u\},\pi_u))) = N^{-u}\sum_{k_1\neq j}\sum_{k_2\neq j,k_1}\cdots\sum_{k_u\neq j,k_1,\ldots,k_{u-1}}\prod_{z=1}^{u} F^{p_z}_{jk_z} \\ &= N^{-u}\sum_{k_1\neq j}{\sum_{k_2\neq j}}'\cdots{\sum_{k_u\neq j}}'\prod_{z=1}^{u} F^{p_z}_{jk_z} < N^{-u}{\sum_{k_1\neq j}}'\cdots{\sum_{k_u\neq j}}' F^{p_1}_{jk_1}\ldots F^{p_i-2}_{jk_i}\ldots F^{p_u}_{jk_u} \times N^{2/D}F^2_{\min}. \end{aligned} \tag{F4}$$

For $D = 2$, $E'[F^2] \to N^{-1}\sum_{k\neq j} F^2_{jk} \sim \ln(N)/N$, while $F^2_{\min} \sim 1/N$, meaning that $F^2_{\min} <_N E'[F^2]$ and therefore $N^{2/D}F^2_{\min} <_N NE'[F^2]$. For $D = 3$, $E'[F^2] \sim N^{-2/3}$ while $F^2_{\min} \sim N^{-2/D} = N^{-2/3}$, so $F^2_{\min} \sim E'[F^2]$, and therefore

$N^{2/D}F_{\min}^2 <_N NE'[F^2]$. Using this, and the fact that for any unique $k_1 \ldots k_u$, $\sum_{k\neq j} F_{jk}^2 \to \sum_{k\neq j,k_1,\ldots,k_u} F_{jk}^2$,

$$\begin{aligned}
&N^{-u}\sum_{k_1\neq j}\cdots\sum_{k_u\neq j}{}' F_{jk_1}^{p_1}\ldots F_{jk_i}^{p_i-2}\ldots F_{jk_u}^{p_u}\times N^{2/D}F_{\min}^2\\
&<_N N^{1-u}\sum_{k_1\neq j}\cdots\sum_{k_u\neq j}{}' F_{jk_1}^{p_1}\ldots F_{jk_i}^{p_i-2}\ldots F_{jk_u}^{p_u}\sum_{k_{u+1}\neq j}F_{jk_{u+1}}^2/N\\
&\to N^{1-u}\sum_{k_1\neq j}\cdots\sum_{k_u\neq j}{}' F_{jk_1}^{p_1}\ldots F_{jk_i}^{p_i-2}\ldots F_{jk_u}^{p_u}\sum_{k_{u+1}\neq j}{}' F_{jk_{u+1}}^2/N\\
&= N^{-u}\sum_{k_1\neq j}\cdots\sum_{k_{u+1}\neq j}{}' F_{jk_1}^{p_1}\ldots F_{jk_u}^{p_u}F_{jk_{u+1}}^2 = NE'_{s'}\Big[\prod F\Big].
\end{aligned}\tag{F5}$$

thus establishing the desired result for $D=2$ and $D=3$.

For the single-qubit case, we show that $E'_{(2,m)}[\prod F]\to E'[F^2]^{m/2}$, where $E'_{(2,m)}[\prod F]$ is defined in Appendix B and also below for any even integer m. We begin by rewriting $E'_{(2,m)}[\prod F]$:

$$\begin{aligned}
E'_{(2,m)}\Big[\prod F\Big] &\to N^{-m/2}\sum_{k_1\neq j}\sum_{k_2\neq j}{}'\cdots\sum_{k_{m/2}\neq j}{}' F_{jk_1}^2F_{jk_2}^2\ldots F_{jk_{m/2}}^2\\
&= N^{-m/2}\sum_{k_1\neq j}\cdots\sum_{k_{m/2-1}\neq j}{}' F_{jk_1}^2\ldots F_{jk_{m/2-1}}^2\left(\sum_{k_{m/2}\neq j}F_{jk_{m/2}}^2-\sum_{i=1}^{m/2-1}F_{jk_i}^2\right).
\end{aligned}\tag{F6}$$

Let us compare the size of the two terms; the first, $N^{-m/2}\sum_{k_1\neq j}\cdots\sum'_{k_{m/2-1}\neq j}F_{jk_1}^2\ldots F_{jk_{m/2-1}}^2\sum_{k_{m/2}\neq j}F_{jk_{m/2}}^2$, is equal to $E'_{(2,m-2)}[\prod F]E'[F^2]$. The second, $N^{-m/2}\sum_{k_1\neq j}\cdots\sum'_{k_{m/2-1}\neq j}F_{jk_1}^2\ldots F_{jk_{m/2-1}}^2\sum_{i=1}^{m/2-1}F_{jk_i}^2$, is less than $N^{-m/2}\sum_{k_1\neq j}\cdots\sum'_{k_{m/2-1}\neq j}F_{jk_1}^2\ldots F_{jk_{m/2-1}}^2\times(m/2-1)F_{\max}^2=(m/2-1)E'_{(2,m-2)}[\prod F]F_{\max}^2/N$. In both two and three dimensions, $(m-1)F_{\max}^2/N\sim N^{-1}<_N E'[F^2]$, so the second term is negligible compared to the first for large N and thus $E'_{(2,m)}[\prod F]\to E'_{(2,m-2)}[(F^2)^{m-1}]E'[F^2]$. The base case $E'_{(2,2)}[\prod F]=E'[F^2]$ is true by definition, and so by induction $E'_{(2,m)}[\prod F]\to E'[F^2]^{m/2}$ for all even integers m.

For the full Hamiltonian case, we first show that $E_s[|\prod F|]<NE_{s'}[|\prod F|]$ when s is a pattern in which there exists a pair of subsets whose intersection has more than two elements, and s' is the pattern created from s by removing two of the elements contained in the intersect of such a pair of subsets in s from both of those subsets, and adding two new subsets, each of which contains the two removed elements. To do this, let us define an intermediate pattern, s'', which is s but with the two elements moved to two new subsets by s' instead of simply removed from both subsets in which they originally appeared in s. Thus for $s\in\mathcal{S}_m(u,v)$, $s''\in\mathcal{S}_{m-2}(u,v)$ and $s'\in\mathcal{S}_m(u',v')=\mathcal{S}_m(u+2,v')$. Using the inequality established above, that for any k and l, $F_{kl}\leqslant N^{1/2}F_{\min}$, and again using $\sum'_{k_i}=\sum_{k_i\neq k_1,\ldots,k_{i-1}}$, we obtain the desired result:

$$\begin{aligned}
E_s\Big[\Big|\prod F\Big|\Big] &\to N^{-u}\sum_{(k_1\ldots k_u)}^{(\mathcal{N})}\sum_{\pi_u}\Big|\prod F(K(s,L(\{k_1\ldots k_u\},\pi_u)))\Big|\\
&< N^{-u}\sum_{(k_1\ldots k_u)}^{(\mathcal{N})}\sum_{\pi_u}\Big|\prod F(K(s'',L(\{k_1\ldots k_u\},\pi_u)))\Big|\times N^{2/D}F_{\min}^2\\
&< N^{2/D-u}\sum_{(k_1\ldots k_u)}^{(\mathcal{N})}\sum_{\pi_u}\Big|\prod F(K(s'',L(\{k_1\ldots k_u\},\pi_u)))\Big|\frac{\sum_{k_{u+1}\neq k_1,\ldots,k_u}\sum_{k_{u+2}\neq k_1,\ldots,k_{u+1}}F_{k_{u+1}k_{u+2}}^2}{(N-u)(N-u-1)}\\
&= N^{2/D-u}\sum_{(k_1\ldots k_u)}^{(\mathcal{N})}\sum_{\pi_u}\Big|\prod F(K(s'',L(\{k_1\ldots k_u\},\pi_u)))\Big|\frac{\sum'_{k_{u+1}}\sum'_{k_{u+2}}F_{k_{u+1}k_{u+2}}^2}{(N-u)(N-u-1)}\\
&\to N^{2/D-2-u}\sum_{(k_1\ldots k_{u+2})}^{(\mathcal{N})}\Big|\prod_{\pi_{u+2}}F(K(s',L(\{k_1\ldots k_{u+2}\},\pi_{u+2}))\Big| = N^{2/D}E_{s'}\Big[\Big|\prod F\Big|\Big],
\end{aligned}\tag{F7}$$

and therefore, for both $D=2$ and $D=3$,

$$E_s\Big[\Big|\prod F\Big|\Big]<NE_{s'}\Big[\Big|\prod F\Big|\Big].\tag{F8}$$

Next, we show that if $s \in \mathcal{S}_m(u,v)$ has a subset with four or more elements, and its intersect with another subset contains two elements, then for $s' \in \mathcal{S}_m(u',v')$ which is s but with the two elements in the intersect between the two subsets in question removed from both subsets, and both added to each of two new subsets which contains only these two elements, then $E_s[|\prod F|] <_N N E_{s'}[|\prod F|]$. This is done similarly to above, but in order to have $<_N$ instead of $<$, we use the fact that in $D=2$, $E[F^2] \to N^{-2}\sum_k \sum_{l\neq k} F_{kl}^2 \sim \ln(N)/N$ and $F_{\min}^2 \sim 1/N$, while in $D=3$, $E[F^2] \sim N^{-2/3}$ and $F_{\min}^2 \sim N^{-2/3}$, meaning that in either case $N^{2/D}F_{\min}^2 <_N NE[F^2]$. Additionally, we use that, for any finite set of u qubits $k_1,\ldots,k_u$, $\sum_{k_{u+1}\neq k_1,\ldots,k_u}\sum_{k_{u+2}\neq k_1,\ldots,k_{u+1}} F_{k_{u_1}k_{u+2}}^2 = \sum'_{k_{u+1}}\sum'_{k_{u+2}} F_{k_{u_1}k_{u+2}}^2 \to \sum_{k_{u+1}}\sum_{k_{u+2}\neq k_{u+1}} F_{k_{u+1}k_{u+2}}^2 \to N^2E[F^2]$. Let $s'' \in \mathcal{S}_{m-2}(u'',v'')$ be s but with the two elements moved to new subsets in s' simply removed from both subsets they appear in. We must treat the case that both subsets with an intersect with two elements have four or more elements, as well as the case when one has four or more and the other has two. In the former case, $u''=u$ and $u'=u+2$, and we have

$$\begin{aligned}
E_s\Big[\Big|\prod F\Big|\Big] &\to N^{-u}\sum_{(k_1\ldots k_u)}^{(\mathcal{N})}\sum_{\pi_u}\Big|\prod F(K(s,L(\{k_1\ldots k_u\},\pi_u)))\Big| \\
&< N^{-u}\sum_{(k_1\ldots k_u)}^{(\mathcal{N})}\sum_{\pi_u}\Big|\prod F(K(s'',L(\{k_1\ldots k_u\},\pi_u)))\Big| \times N^{2/D}F_{\min}^2 \\
&<_N N^{1-u}\sum_{(k_1\ldots k_u)}^{(\mathcal{N})}\sum_{\pi_u}\Big|\prod F(K(s'',L(\{k_1\ldots k_u\},\pi_u)))\Big| \times E(F^2) \\
&\to N^{-1-u}\sum_{(k_1\ldots k_u)}^{(\mathcal{N})}\sum_{\pi_u}\Big|\prod F(K(s'',L(\{k_1\ldots k_u\},\pi_u)))\Big|\sum_{k_{u+1}}{}'\sum_{k_{u+2}}{}' F_{k_{u+1}k_{u+2}}^2 \\
&= N^{-1-u}\sum_{(k_1\ldots k_{u+2})}^{(\mathcal{N})}\Big|\prod_{\pi_{u+2}} F(K(s',L(\{k_1\ldots k_{u+2}\}),\pi_{u+2}))\Big| = NE_{s'}\Big[\Big|\prod F\Big|\Big].
\end{aligned} \tag{F9}$$

If one of the subsets has only two elements, then $u''=u-1$ and $u'=u+1$, so

$$\begin{aligned}
E_s\Big[\Big|\prod F\Big|\Big] &\to N^{-u}\sum_{(k_1\ldots k_u)}^{(\mathcal{N})}\sum_{\pi_u}\Big|\prod F(K(s,L(\{k_1\ldots k_u\},\pi_u)))\Big| \\
&< N^{-u}(N-(u-1))\sum_{(k_1\ldots k_{u-1})}^{(\mathcal{N})}\sum_{\pi_{u-1}}\Big|\prod F(K(s'',L(\{k_1\ldots k_{u-1}\},\pi_{u-1})))\Big| \times N^{2/D}F_{\min}^2 \\
&\to N^{1-u}\sum_{(k_1\ldots k_{u-1})}^{(\mathcal{N})}\sum_{\pi_{u-1}}\Big|\prod F(K(s'',L(\{k_1\ldots k_{u-1}\},\pi_{u-1})))\Big| \times N^{2/D}F_{\min}^2 \\
&<_N N^{2-u}\sum_{(k_1\ldots k_{u-1})}^{(\mathcal{N})}\sum_{\pi_{u-1}}\Big|\prod F(K(s'',L(\{k_1\ldots k_{u-1}\},\pi_{u-1})))\Big| \times E(F^2) \\
&\to N^{-u}\sum_{(k_1\ldots k_{u-1})}^{(\mathcal{N})}\sum_{\pi_{u-1}}\Big|\prod F(K(s'',L(\{k_1\ldots k_{u-1}\},\pi_{u-1})))\Big|\sum_{k_u}{}'\sum_{k_{u+1}}{}' F_{k_uk_{u+1}}^2 \\
&= N^{-u}\sum_{(k_1\ldots k_{u+1})}^{(\mathcal{N})}\Big|\prod_{\pi_{u+1}} F(K(s',L(\{k_1\ldots k_{u+1}\},\pi_{u+1})))\Big| = NE_{s'}\Big[\Big|\prod F\Big|\Big].
\end{aligned} \tag{F10}$$

Thus in both cases, which are exhaustive, we have established the desired result.

For m even, we show that if $s \in \mathcal{S}_m(u,v)$ has $u-v=2a$ subsets with two elements and the property that the intersect between any of these subsets with any other is two or zero (there must be an even number of these), and the other v subsets, which contain a total of $m-2a=b$ integers, have intersects with all other subsets which contain no more than one element, and s' is a pattern where all subsets have two elements and all intersects have two or zero elements (i.e., $b=0$), then for $b\neq 0$, $E_s[|\prod F|] < N^{b/2-1/2}E_{s'}[|\prod F|]$. All s' of this form have the same expectation value, which we denote $E_{s'}[|\prod F|] = E_{(2,m)}[|\prod F|]$. Let $s'' \in \mathcal{S}_{2a}(2a,0)$ be s but with all subsets which with an intersect with another subset containing one element removed, so that

$u'' = u - v$:

$$
\begin{aligned}
E_s\Big[\Big|\prod F\Big|\Big] &\to N^{-u} \sum_{(k_1 \ldots k_u)}^{(\mathcal{N})} \sum_{\pi_u} \Big| \prod F(K(s, L(\{k_1 \ldots k_u\}, \pi_u))) \Big| \\
&< N^{-u} N^{v-2} \sum_{(k_1 \ldots k_{u-v})}^{(\mathcal{N})} \sum_{\pi_{u-v}} \Big| \prod F(K(s'', L(\{k_1 \ldots k_{u-v}\}, \pi_{u-v}))) \Big| \\
&\quad \times \sum_{k_{u-v+1}}{}' \sum_{k_{u-v+2}}{}' \Big| F_{k_{u-v+1} k_{u-v+2}} \Big| N^{(b-1)/D} F_{\min}^{b-1} \\
&< N^{v-2-u+(b-1)/D} \sum_{(k_1 \ldots k_{u-v})}^{(\mathcal{N})} \sum_{\pi_{u-v}} \Big| \prod F(K(s'', L(\{k_1 \ldots k_{u-v}\}, \pi_{u-v}))) \Big| \\
&\quad \times \frac{\sum'_{k_{u-v+1}} \ldots \sum'_{k_{u-v+b}} F^2_{k_{u-v+1} k_{u-v+2}} \ldots F^2_{k_{u-v+b-1} k_{u-v+b}}}{(N - (u-v+2))(N - (u-v+3)) \ldots (N - (u-v+(b-1)))} \\
&\to N^{v-2-u+(b-1)/D} \sum_{(k_1 \ldots k_{u-v})}^{(\mathcal{N})} \sum_{\pi_{u-v}} \Big| \prod F(K(s'', L(\{k_1 \ldots k_{u-v}\}, \pi_{u-v}))) \Big| \\
&\quad \times N^{-(b-2)} \sum_{k_{u-v+1}}{}' \ldots \sum_{k_{u-v+b}}{}' F^2_{k_{u-v+1} k_{u-v+2}} \ldots F^2_{k_{u-v+b-1} k_{u-v+b}} \\
&= N^{v-u+b/D-1/D-b} \sum_{(k_1 \ldots k_{u-v+b})} \sum_{\pi_{u-v+b}} \Big| \prod F(K(s', L(\{k_1 \ldots k_{u-v+b}\}, \pi_{u-v+b}))) \Big| \\
&\to N^{v-u-b/D-1/D+m} E_{s'}\Big[\Big| \prod F \Big|\Big] = N^{(b-1)/D} E_{s'}\Big[\Big|\prod F\Big|\Big],
\end{aligned} \tag{F11}
$$

since $u - v + b = u - v + m - 2a = m$. $(b-1)/3 < (b-1)/2$, so for $D = 2$ or $D = 3$,

$$
E_s\Big[\Big|\prod F\Big|\Big] < N^{b/2-1/2} E_{s'}\Big[\prod F\Big]. \tag{F12}
$$

For m odd, we show that if $s \in \mathcal{S}_m(u,v)$ has $u - v = 2a$ subsets with two elements and the property that the intersect between any of these subsets with any other is two or zero (there must be an even number of these), and the other v subsets, which contain a total of $m - 2a = b$ integers, have intersects with all other subsets which contain no more than one element, and s' is a pattern where all subsets but three have two elements and all intersects between these subsets contain two or zero elements and the other three subsets each contain two elements and the intersect between any two of them contains one element (i.e., s but with $b = 3$), then for $b \geqslant 5$, $E_s[|\prod F|] <_N N^{b/2-3/2} E_{s'}[|\prod F|]$. All s' of this form have the same expectation value, which we denote $E_{s'}[|\prod F|] = E_{(3,m)}[|\prod F|]$. Again, let $s'' \in \mathcal{S}_{2a}(2a, 0)$ be s but with all subsets which with an intersect with another subset containing one element removed, so that $u'' = u - v$:

$$
\begin{aligned}
E_s\Big[\Big|\prod F\Big|\Big] &\to N^{-u} \sum_{(k_1 \ldots k_u)}^{(\mathcal{N})} \sum_{\pi_u} \Big| \prod F(K(s, L(\{k_1 \ldots k_u\}, \pi_u))) \Big| \\
&< N^{-u} N^{v-5} \sum_{(k_1 \ldots k_{u-v})}^{(\mathcal{N})} \sum_{\pi_{u-v}} \prod F(K(s'', L(\{k_1 \ldots k_{u-v}\}, \pi_{u-v}))) \\
&\quad \times \sum_{k_{u-v+1}}{}' \sum_{k_{u-v+2}}{}' \sum_{k_{u-v+3}}{}' \sum_{k_{u-v+4}}{}' \sum_{k_{u-v+5}}{}' \Big| F_{k_{u-v+1} k_{u-v+2}} F_{k_{u-v+2} k_{u-v+3}} F_{k_{u-v+4} k_{u-v+5}} \Big| N^{(b-3)/D} F_{\min}^{b-3} \\
&< N^{v-5-u+b/D-3/D} \sum_{(k_1 \ldots k_{u-v})}^{(\mathcal{N})} \sum_{\pi_{u-v}} \prod F(K(s'', L(\{k_1 \ldots k_{u-v}\}, \pi_{u-v}))) \\
&\quad \times N^{-(b-5)} \sum_{k_{u-v+1}}{}' \ldots \sum_{k_{u-v+b}}{}' F^2_{k_{u-v+1} k_{u-v+2}} \ldots F^2_{k_{u-v+b-4} k_{u-v+b-3}} \Big| F_{k_{u-v+b-2} k_{u-v+b-1}} F_{k_{u-v-1} k_{u-v}} F_{k_{u-v} k_{u-v-2}} \Big| \\
&= N^{v-u-b+b/D-3/D} \sum_{(k_1 \ldots k_{u-v+b})} \sum_{\pi_{u-v+b}} \prod F(K(s', L(\{k_1 \ldots k_{u-v+b}\}, \pi_{u-v+b}))) \\
&\to N^{v-u-b+b/D-3/D+m} E_{s'}\left(\Big| \prod F \Big|\right) = N^{(b-3)/D} E_{s'}\Big[\Big|\prod F\Big|\Big],
\end{aligned} \tag{F13}
$$

and again, because $(b-3)/3 < (b-3)/2$,

$$E_s\left[\left|\prod F\right|\right] < N^{b/2-3/2} E_{s'}\left[\left|\prod F\right|\right]. \tag{F14}$$

Finally, we simplify $E_{(2,m)}[\prod F]$ and $E_{(3,m)}[\prod F]$ (as defined in Appendix B) in terms of $E[F^2]$ and $E[F^3]$. We begin with showing that $E_{(2,m)}(\prod F) \to E[F^2]^{m/2}$. This is done similarly to the analogous result in the single qubit case. We begin by rewriting $E_{(2,m)}[F]$:

$$\begin{aligned} E_{(2,m)}[F] &\to N^{-m} \sum_{k_1}\sum_{k_2}{}' \cdots \sum_{k_m}{}' F_{k_1k_2}^2 \cdots F_{k_{m-1}k_m}^2 \\ &= N^{-m} \sum_{k_1}\sum_{k_2}{}' \cdots \sum_{k_{m-2}}{}' F_{k_1k_2}^2 \cdots F_{k_{m-3}k_{m-2}}^2 \left(\sum_{k_{m-1}} \sum_{k_m \neq k_{m-1}} F_{k_{m-1}k_m}^2 - \sum_{i=1}^{m-2} \sum_{k \neq k_i} F_{k_i k}^2 - \sum_{i=1}^{m-2} \sum_{k}{}' F_{kk_i}^2 \right). \end{aligned} \tag{F15}$$

Let us compare the size of all three of these terms: The first term, $N^{-m} \sum_{k_1} \sum_{k_2}' \cdots \sum_{k_{m-2}}' F_{k_1k_2}^2 \cdots F_{k_{m-3}k_{m-2}}^2 \sum_{k_{m-1}} \sum_{k_m \neq k_{m-1}} F_{k_{m-1}k_m}^2$, is equal to $E_{(2,m-2)}[\prod F] \times E[F^2]$. The second, $N^{-m} \sum_{k_1} \sum_{k_2}' \cdots \sum_{k_{m-2}}' F_{k_1k_2}^2 \cdots F_{k_{m-3}k_{m-2}}^2 \sum_{i=1}^{m-2} \sum_{k \neq k_i} F_{k_i k}^2$, is smaller than $N^{-m} \sum_{k_1} \sum_{k_2}' \cdots \sum_{k_{m-2}}' F_{k_1k_2}^2 \cdots F_{k_{m-3}k_{m-2}}^2 \times (m-2)(N-1) F_{\max}^2 \to (m-2) F_{\max}^2 E_{(2,m-2)}[\prod F]/N$. Similarly, the third term has the same upper bound for large N. But $(m-2)F_{\max}^2/N \sim N^{-1} <_N E[F^2]$ in both two and three dimensions, so the second and third terms become negligible for large N, and thus $E_{(2,m)}(\prod F) \to E_{(2,m-2)}[\prod F] E[F^2]$. The base case $E_{(2,2)}[\prod F] = E[F^2]$ is true by definition, and so by induction $E_{(2,m)}[\prod F] \to E[F^2]^{m/2}$ for all even integers m.

We now show that the N scaling of $E_{(3,m)}[|\prod F|]$ is at most $E_{(2,m-3)}[\prod F] \times E[|F|]$.

$$\begin{aligned} E_{(3,m)}\left[\left|\prod F\right|\right] &\to N^{-m} \sum_{k_1}\sum_{k_2}{}' \cdots \sum_{k_m}{}' \left| F_{k_1k_2}^2 \cdots F_{k_{m-4}k_{m-3}}^2 F_{k_{m-2}k_{m-1}} F_{k_{m-1}k_m} F_{k_mk_{m-2}} \right| \\ &< N^{-m} \sum_{k_1}\sum_{k_2}{}' \cdots \sum_{k_{m-3}}{}' F_{k_1k_2}^2 \cdots F_{k_{m-4}k_{m-3}}^2 \sum_{k_{m-2}} \sum_{k_{m-1} \neq k_{m-2}} \sum_{k_m \neq k_{m-1}, k_{m-2}} \left| F_{k_{m-2}k_{m-1}} F_{k_{m-1}k_m} F_{k_mk_{m-2}} \right| \\ &< N^{-m} \sum_{k_1}\sum_{k_2}{}' \cdots \sum_{k_{m-3}}{}' F_{k_1k_2}^2 \cdots F_{k_{m-4}k_{m-3}}^2 \sum_{k_{m-2}} \sum_{k_{m-1} \neq k_{m-2}} \sum_{k_m \neq k_{m-1}, k_{m-2}} \left| F_{k_{m-2}k_{m-1}} \right| F_{\max}^2 \\ &< N^{1-m} F_{\max}^2 \sum_{k_1}\sum_{k_2}{}' \cdots \sum_{k_{m-3}}{}' F_{k_1k_2}^2 \cdots F_{k_{m-4}k_{m-3}}^2 \sum_{k} \sum_{l \neq k} |F_{kl}| \\ &\to N^{1-m} F_{\max}^2 \times N^{m-3} E_{(2,m-3)}\left[\prod F\right] \times N^2 E[|F|] \\ &= F_{\max}^2 E_{(2,m-3)}\left[\prod F\right] E[|F|], \end{aligned} \tag{F16}$$

and the result is obtained by noting that $F_{\max} \sim 1$.

[1] M. A. Nielsen and I. L. Chuang, *Quantum Computation and Quantum Information* (Cambridge University Press, Cambridge, UK, 2000).

[2] S. Lloyd, A potentially realizable quantum computer, Science **261**, 1569 (1993).

[3] D. P. DiVincenzo, Quantum computation, Science **270**, 255 (1995).

[4] C. H. Bennett and D. P. DiVincenzo, Quantum information and computation, Nature (London) **404**, 247 (2000).

[5] P. W. Shor, Polynomial-time algorithms for prime factorization and discrete logarithms on a quantum computer, SIAM J. Comp. **26**, 1484 (1997).

[6] A. Ekert and R. Jozsa, Quantum computation and Shor's factoring algorithm, Rev. Mod. Phys. **68**, 733 (1996).

[7] L. K. Grover, Quantum Mechanics Helps in Searching for a Needle in Haystack, Phys. Rev. Lett. **79**, 325 (1997).

[8] D. S. Abrams and S. Lloyd, Quantum Algorithm Providing Exponential Speed Increase for Finding Eigenvalues and Eigenvectors, Phys. Rev. Lett. **83**, 5162 (1999).

[9] C. Monroe, D. M. Meekhof, B. E. King, W. M. Itano, and D. J. Wineland, Demonstration of a Fundamental Quantum Logic Gate, Phys. Rev. Lett. **75**, 4714 (1995).

[10] F. Schmidt-Kaler, H. Häffner, M. Riebe, S. Gulde, G. P. T. Lancaster, T. Deuschle, C. Becher, C. F. Roos, J. Eschner, and R. Blatt, Realization of the Cirac-Zoller controlled-NOT quantum gate, Nature (London) **422**, 408 (2003).

[11] R. Blatt and D. J. Wineland, Entangled states of trapped atomic ions, Nature (London) **453**, 1008 (2008).

[12] D. Schrader, I. Dotsenko, M. Khudaverdyan, Y. Miroshnychenko, A. Rauschenbeutel, and D. Meschede, Neutral Atom Quantum Register, Phys. Rev. Lett. **93**, 150501 (2004).

[13] L. Isenhower, E. Urban, X. L. Zhang, A. T. Gill, T. Henage, T. A. Johnson, T. G. Walker, and M. Saffman, Demonstration of a Neutral Atom Controlled-NOT Quantum Gate, Phys. Rev. Lett. **104**, 010503 (2010).

[14] T. Wilk, A. Gaetan, C. Evellin, J. Wolters, Y. Miroshnychenko, P. Grangier, and A. Browaeys, Entanglement of Two Individual Neutral Atoms Using Rydberg Blockade, Phys. Rev. Lett. **104**, 010502 (2010).

[15] D. Loss and D. P. DiVincenzo, Quantum computation with quantum dots, Phys. Rev. A **57**, 120 (1998).

[16] J. Berezovsky, M. H. Mikkelsen, O. Gywat, N. G. Stoltz, L. A. Cotdren, and D. D. Awschalom, Nondestructive optical measurements of a single electron spin in a quantum dot, Science **314**, 1916 (2006).

[17] A. Wallraff, D. I. Schuster, A. Blais, L. Frunzio, R. S. Huang, J. Majer, S. Kumar, S. M. Girvin, and R. J. Schoelkopf, Strong coupling of a single photon to a superconducting qubit using circuit quantum electrodynamics, Nature (London) **431**, 162 (2004).

[18] J. Clarke and F. K. Wilhelm, Superconducting quantum bits, Nature (London) **453**, 1031 (2008).

[19] E. Knill, R. Laflamme, and G. J. Milburn, A scheme for efficient quantum computation with linear optics, Nature (London) **409**, 46 (2001).

[20] T. B. Pittman, B. C. Jacobs, and J. D. Franson, Demonstration of Nondeterministic Quantum Logic Operations Using Linear Optical Elements, Phys. Rev. Lett. **88**, 257902 (2002).

[21] P. Shor, Scheme for reducing decoherence in quantum computer memory, Phys. Rev. A **52**, R2493(R) (1995).

[22] A. M. Steane, Error Correcting Codes in Quantum Theory, Phys. Rev. Lett. **77**, 793 (1996).

[23] D. Aharonov and M. Ben-Or, in *Fault Tolerant Quantum Computation with Constant Error*, Proceedings of the 29th Annual ACM Symposium on the Theory of Computing (ACM (Association for Computing Machinery), New-York, 1997), p. 176.

[24] B. M. Terhal and G. Burkard, Fault-tolerant quantum computation for local non-Markovian noise, Phys. Rev. A **71**, 012336 (2005).

[25] P. Aliferis, D. Gottesman, and J. Preskill, Quantum accuracy threshold for concatenated distance-3 codes, Quant. Inf. Comput. **6**, 97 (2006).

[26] D. Aharonov, A. Kitaev, and J. Preskill, Fault-Tolerant Quantum Computation with Long-Range Correlated Noise, Phys. Rev. Lett. **96**, 050504 (2006).

[27] H. K. Ng and J. Preskill, Fault-tolerant quantum computation versus Gaussian noise, Phys. Rev. A **79**, 032318 (2009).

[28] J. Preskill, Sufficient condition on noise correlations for scalable quantum computing, Quant. Inf. Comput. **13**, 181 (2013).

[29] A. G. Fowler, M. Mariantoni, J. M. Martinis, and A. N. Cleland, Surface codes: Towards practical large-scale quantum computation, Phys. Rev. A **86**, 032324 (2012).

[30] D. Staudt, The role of correlated noise in quantum computing, arXiv:1111.1417.

[31] M. I. Dyakonov, Is fault-tolerant quantum computation really possible? arXiv:quant-ph/0610117.

[32] R. Alicki, Comment on "Resilient quantum computation in correlated environments: A quantum phase transition perspective" and "Fault-tolerant quantum computation with longe-range correlated noise," arXiv:quant-ph/0702050.

[33] G. Kalai, Detrimental decoherence, arXiv:0806.2443.

[34] D. D. Yavuz, Superradiance as a source of collective decoherence in quantum computers, J. Opt. Soc. Am. B **31**, 2665 (2014).

[35] C. H. Papadimitriou, *Computational Complexity* (Addison-Wesley, New York, 1995).

[36] E. Novais and E. R. Mucciolo, Surface Code Threshold in the Presence of Correlated Errors, Phys. Rev. Lett. **110**, 010502 (2013).

[37] E. Novais, E. R. Mucciolo, and H. U. Baranger, Resilient Quantum Computation in Correlated Environments: A Quantum Phase Transition Perspective, Phys. Rev. Lett. **98**, 040501 (2007).

[38] E. Novais, A. J. Stanforth, and E. R. Mucciolo, Surface code fidelity at finite temperatures, Phys. Rev. A **95**, 042339 (2017).

[39] P. Jouzdani, E. Novais, I. S. Tupitsyn, and E. R. Mucciolo, Fidelity threshold of the surface code beyond single-qubit error models, Phys. Rev. A **90**, 042315 (2014).

[40] A. Hutter and D. Loss, Breakdown of surface-code error correction due to coupling to a bosonic bath, Phys. Rev. A **89**, 042334 (2014).

[41] T. Albash and D. A. Lidar, Adiabatic quantum computing, arXiv:1611.04471 [quant-ph].

[42] C. Nayak, S. H. Simon, A. Stern, M. Freedman, and S. Das Sarma, Non-Abelian anyons and topological quantum computation, Rev. Mod. Phys. **80**, 1083 (2008).

[43] D. A. Lidar, I. L. Chuang, and K. B. Whaley, Decoherence Free Subspaces for Quantum Computation, Phys. Rev. Lett. **81**, 2594 (1998).

[44] D. A. Lidar, D. Bacon, and K. B. Whaley, Concatenating Decoherence-Free Subspaces with Quantum Error Correcting Codes, Phys. Rev. Lett. **82**, 4556 (1999).

[45] J. Kempe, D. Bacon, D. A. Lidar, and K. B. Whaley, Theory of decoherence-free fault-tolerant universal quantum computation, Phys. Rev. A **63**, 042307 (2001).

[46] R. I. Karasik, K. P. Marzlin, B. C. Sanders, and K. B. Whaley, Multiparticle decoherence-free subspaces in extended systems, Phys. Rev. A **76**, 012331 (2007).

[47] R. H. Dicke, Coherence in spontaneous radiation processes, Phys. Rev. **93**, 99 (1954).

[48] M. Gross and S. Haroche, Superradiance: An essay on the theory of collective spontaneous emission, Phys. Rep. **93**, 301 (1982).

[49] T. Wang and S. F. Yelin, Theory for Raman superradiance in atomic gases, Phys. Rev. A **72**, 043804 (2005).

[50] E. Wolfe and S. F. Yelin, Certifying Separability in Symmetric Mixed States of N Qubits, and Superradiance, Phys. Rev. Lett. **112**, 140402 (2014).

[51] R. T. Sutherland and F. Robicheaux, Coherent forward broadening in cold atom clouds, Phys. Rev. A **93**, 023407 (2016).

[52] R. T. Sutherland and F. Robicheaux, Superradiance in inverted multilevel atomic clouds, Phys. Rev. A **95**, 033839 (2017).

[53] N. Ghazanfari and O. E. Mustecaplioglu, Acoustic superradiance from an optical-superradiance-induced vortex in a Bose-Einstein condensate, Phys. Rev. A **89**, 043619 (2014).

[54] O. E. Mustecaplioglu and L. You, Superradiant light scattering from trapped Bose-Einstein condensates, Phys. Rev. A **62**, 063615 (2000).

[55] M. O. Araujo, I. Kresic, R. Kaiser, and W. Guerin, Superradiance in a Large and Dilute Cloud of Cold Atoms in the Linear-Optics Regime, Phys. Rev. Lett. **117**, 073002 (2016).

[56] S. J. Roof, K. J. Kemp, M. D. Havey, and I. M. Sokolov, Observation of Single-Photon Superradiance and the Cooperative Lamb Shift in an Extended Sample of Cold Atoms, Phys. Rev. Lett. **117**, 073003 (2016).

[57] T. Hill, B. C. Sanders, and H. Deng, Cooperative light scattering in any dimension, Phys. Rev. A **95**, 033832 (2017).

[58] J. J. Choquette, K. P. Marzlin, and B. C. Sanders, Superradiance, subradiance, and suppressed superradiance of dipoles near a metal interface, Phys. Rev. A **82**, 023827 (2010).

[59] S. Utsunomiya, C. P. Master, and Y. Yamamoto, Algorithm-based analysis of collective decoherence in quantum computation, J. Opt. Soc. Am. B **24**, 198 (2007).

[60] I. M. Sokolov, M. D. Kupriyanova, D. V. Kupriyanov, and M. D. Havey, Light scattering from a dense and ultracold atomic gas, Phys. Rev. A **79**, 053405 (2009).

[61] I. E. Mazets and G. Kurizki, Multi-atom coooperative emission following single photon absorption: Dicke-State dynamics, J. Phys. B: At. Mol. Opt. Phys. **40**, F105 (2007).

[62] L. H. Pedersen and K. Molmer, Few qubit atom-light interfaces with collective encoding, Phys. Rev. A **79**, 012320 (2009).

[63] Y. Yamamoto and A. Imamoglu, *Mesoscopic Quantum Optics* (John Wiley & Sons, New York, 1999).

[64] D. A. Cheng, *Field and Wave Electromagnetics* (Addison-Wesley, New York, 1989).

[65] A. Papoulis, *Probability, Random Variables, and Stochastic Processes* (McGraw-Hill, New York, 1965).

[66] F. Barahona, On the computational complexity of Ising spin-glass models, J. Phys. A **15**, 3241 (1982).

[67] D. L. Stein and C. M. Newman, Spin glasses: Old and new complexity, Complex Sys. **20**, 115 (2011).

[68] K. R. A. Hazzard, M. van den Worm, M. Foss-Feig, S. R. Manmana, E. G. Dalla-Tore, T. Pfau, M. Kastner, and A. M. Rey, Quantum correlations and entanglement in far-from-equilibrium spin systems, Phys. Rev. A. **90**, 063622 (2014).